Planetary boundary layer and atmospheric turbulence.

Szymon P. Malinowski
Marta Wacławczyk

Institute of Geophysics UW

2017/18

Lecture 09

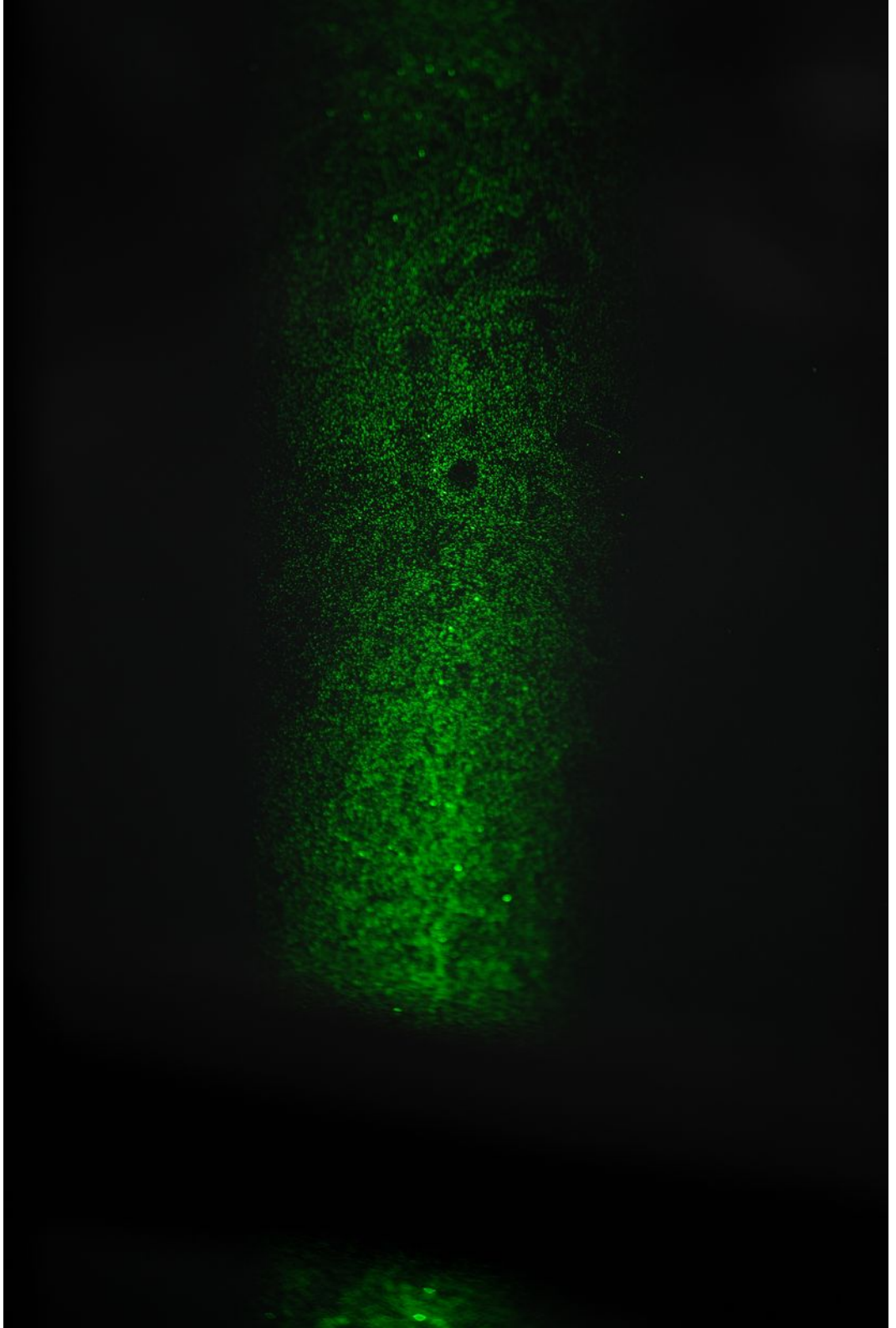

What is cloud?

Cloud – A visible aggregate of minute water droplets and/or ice particles in the atmosphere above the earth's surface

Glossary of Meteorology, 2000
American Meteorological Society

Cloud – any visible mass of water droplets, or ice crystals, or a mixture of both that is suspended in the air, usually at a considerable height

The New Encyclopedia Britannica, 1998

What is the typical size of aerosol particles ?

From a few nanometers: a few molecules condensed
To a few centimeters: hailstones

Stokes law, (after Vaillancourt and Yau, 2000):

Particles, assumed spherical, are essentially described by their mass (m_p) and radius (R). With these two parameters, and the dynamic viscosity of the carrier fluid, μ, we can calculate the particle's response time τ_P (also called the relaxation or Stokes timescale).
The timescale τ_P is the characteristic time the particle takes to react to changes in the flow. For particles with density much larger than that of the surrounding fluid and small Reynolds number the equation of motion involves only the drag force and gravity. When there is no motion in the fluid, the solution of the equation of motion of the particle is:

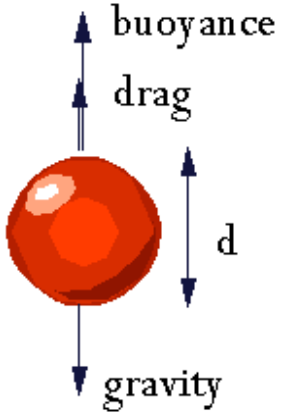

$$V(t) = V_T\,[1 - exp(-t/\tau_p)],$$

where $V_T = \tau_P\, g$ is the particle's terminal velocity (or drift velocity or Stokes settling velocity) and

$$\tau_P = m_p/(6\pi R\mu) = 2\rho_w R^2/9\mu$$

is the time for the velocity of the particle to reach about 63% $[1 - (1/exp)]$ of its terminal velocity.
The symbol ρ_w denotes the density of water and g is the gravitational acceleration.

The following four dimensionless parameters are useful to predict the nature or degree of the particle–flow mechanical coupling of individual particles or the overall effect of a group of particles on the flow:

- the ratio d/l, where d is the particle diameter and l is a characteristic length scale of the flow [either the Kolmogorov length scale (η) or the integral scale (L)];

For $d/\eta << 1$, the diameter of the particles is much smaller than the Kolmogorov length scale, and the particles will exert no direct influence on the kinematic fields.

For $d/L \sim 1$, the particle is of the same size as that of the energy containing eddies, so the particles are expected to have a significant direct impact on the kinematic fields.

- the particle's Reynolds number, $Re_P = UR/v$, where U is the relative velocity between the flow and the particle, R is the radius of the particle, and v is the kinematic viscosity of the fluid;

The particle's Reynolds number is important because particles with large Reynolds number influence directly the turbulent kinetic energy through vortex shedding.

- the Stokes number, which is the ratio between the particle's response time (τ_P) and a characteristic timescale of the flow (τ_F),

$$St = \tau_P/\tau_F;$$

Small Stokes number: particles react almost instantaneously to any accelerations of the flow, they behave as a tracer.

Stokes number close to 1: maximum interaction between the flow and the particles.

Large Stokes number: particles respond very slowly to the accelerations in the flow, the spatial distribution of the particles is independent from the flow.

- the mass loading (M_P/M_F), that is, the ratio of the total mass of particles (M_P) and the mass of the carrier fluid (M_F).

Small mass loading - the overall effect of particles negligible.

Appreciable mass loading – influence on the flow important.

CLOUD-PARTICLE FALLSPEEDS

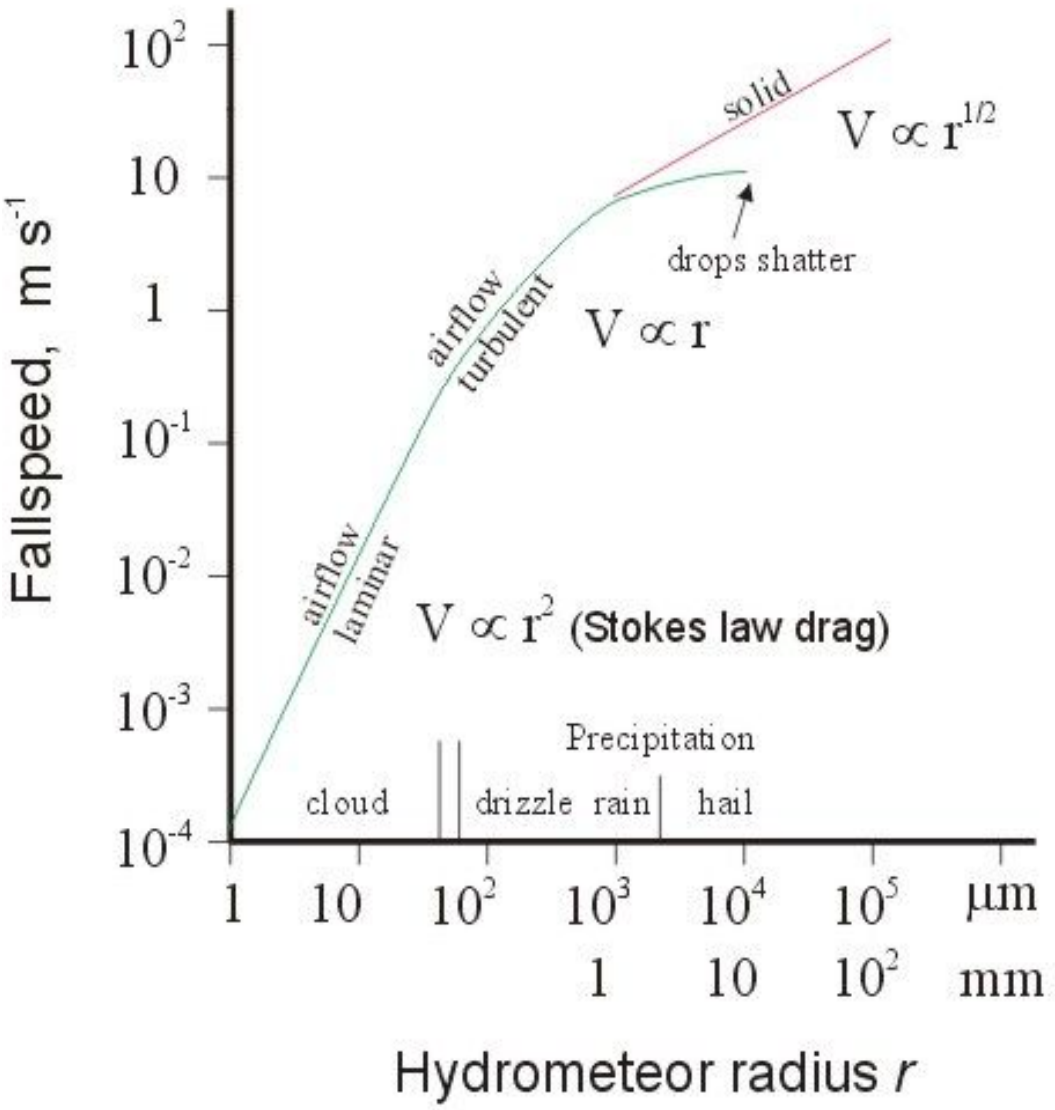

Terminal (equilibrium) fall speeds of particles
(solid spheres and droplets):

gravity = drag

Adapted from McIlveen (1992)

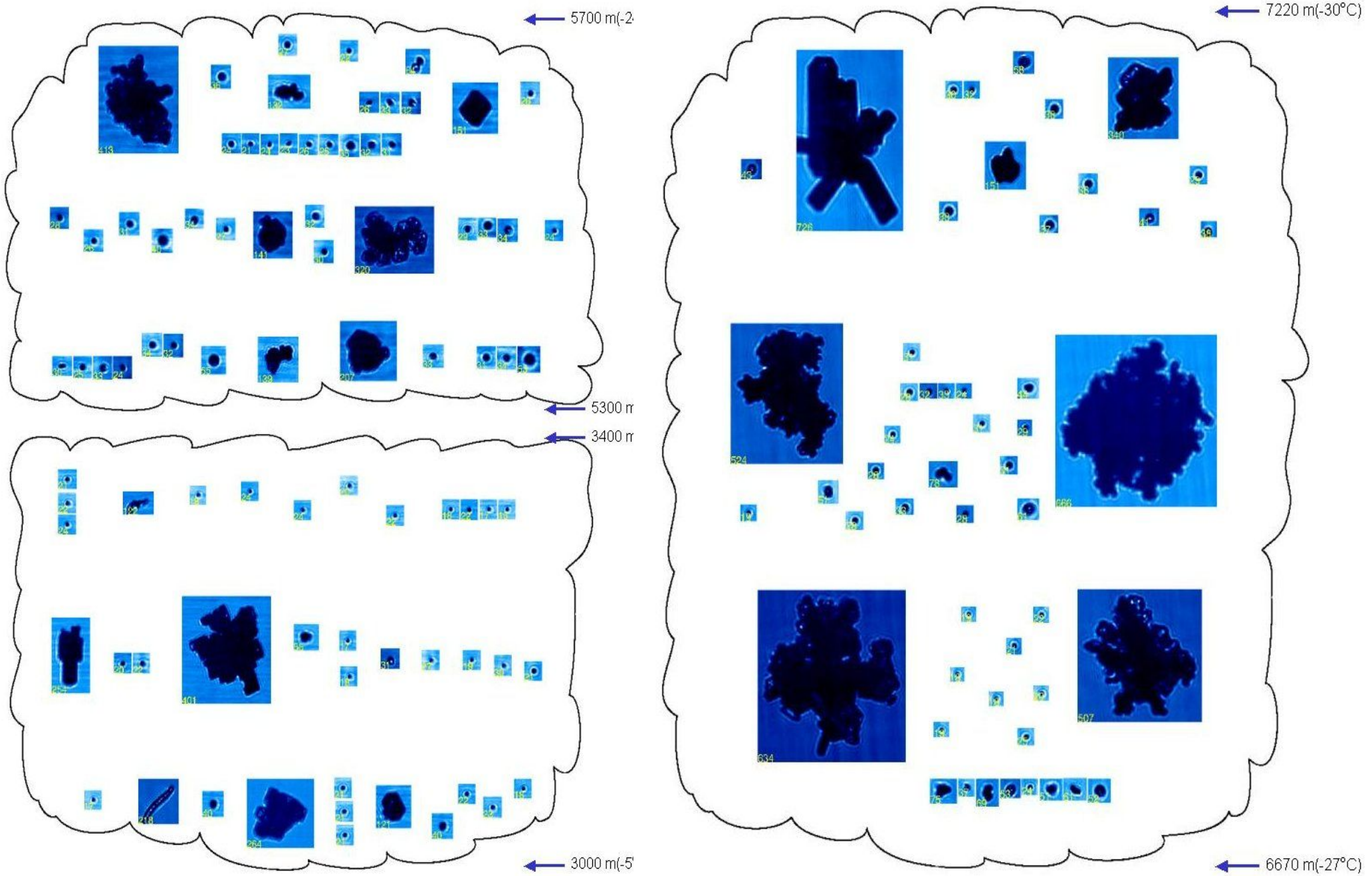

Cloud particles at various heights (temperatures) imaged by CPI (SPEC Inc.)

Inertial cloud particles:
cloud condensation nuclei, cloud droplets, ice particles, Inertial Inertial precipitation particles: snow, hail, rain, graupel, drizzle....

Source: Universitat Bonn

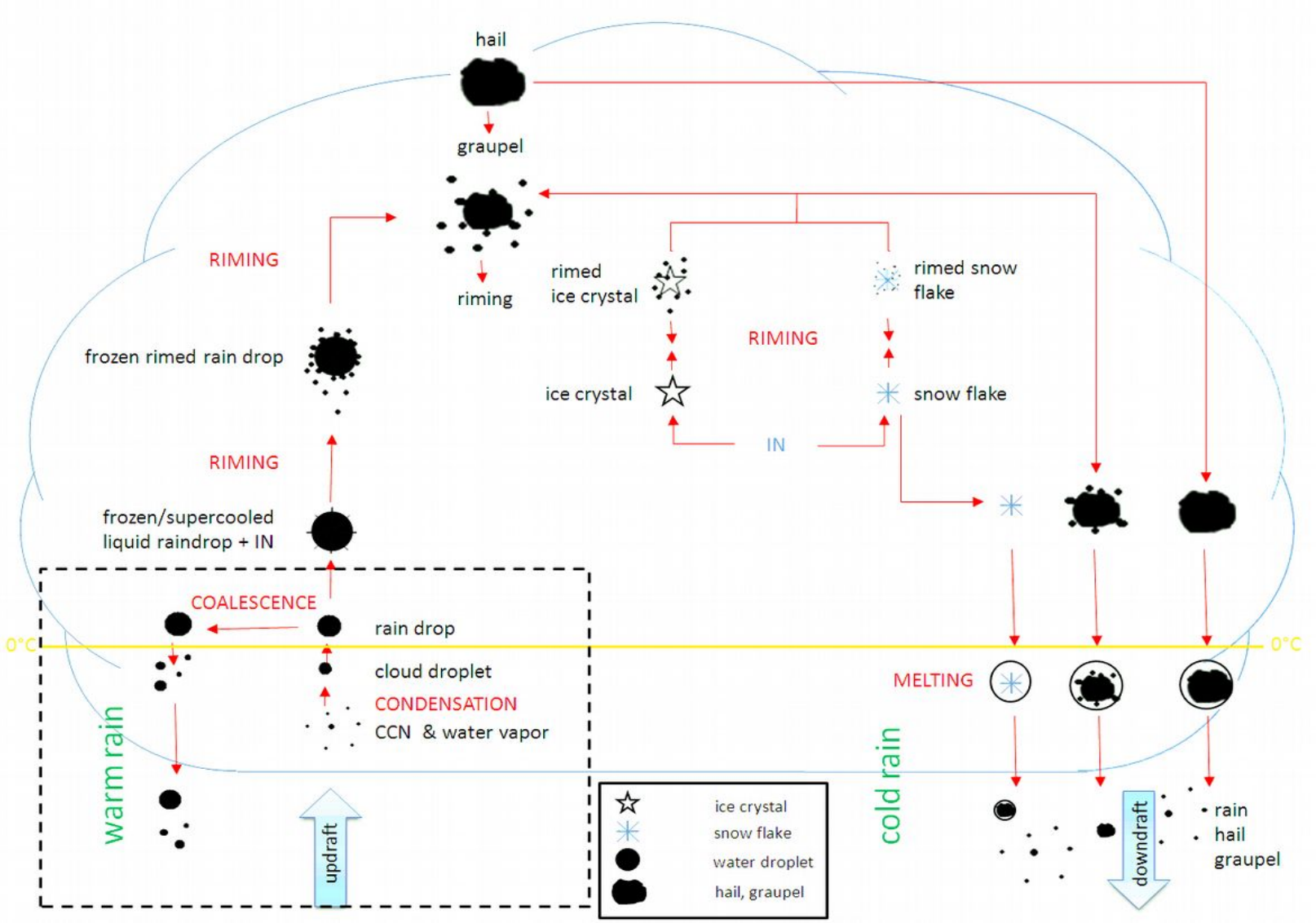

Aerosol and cloud particles

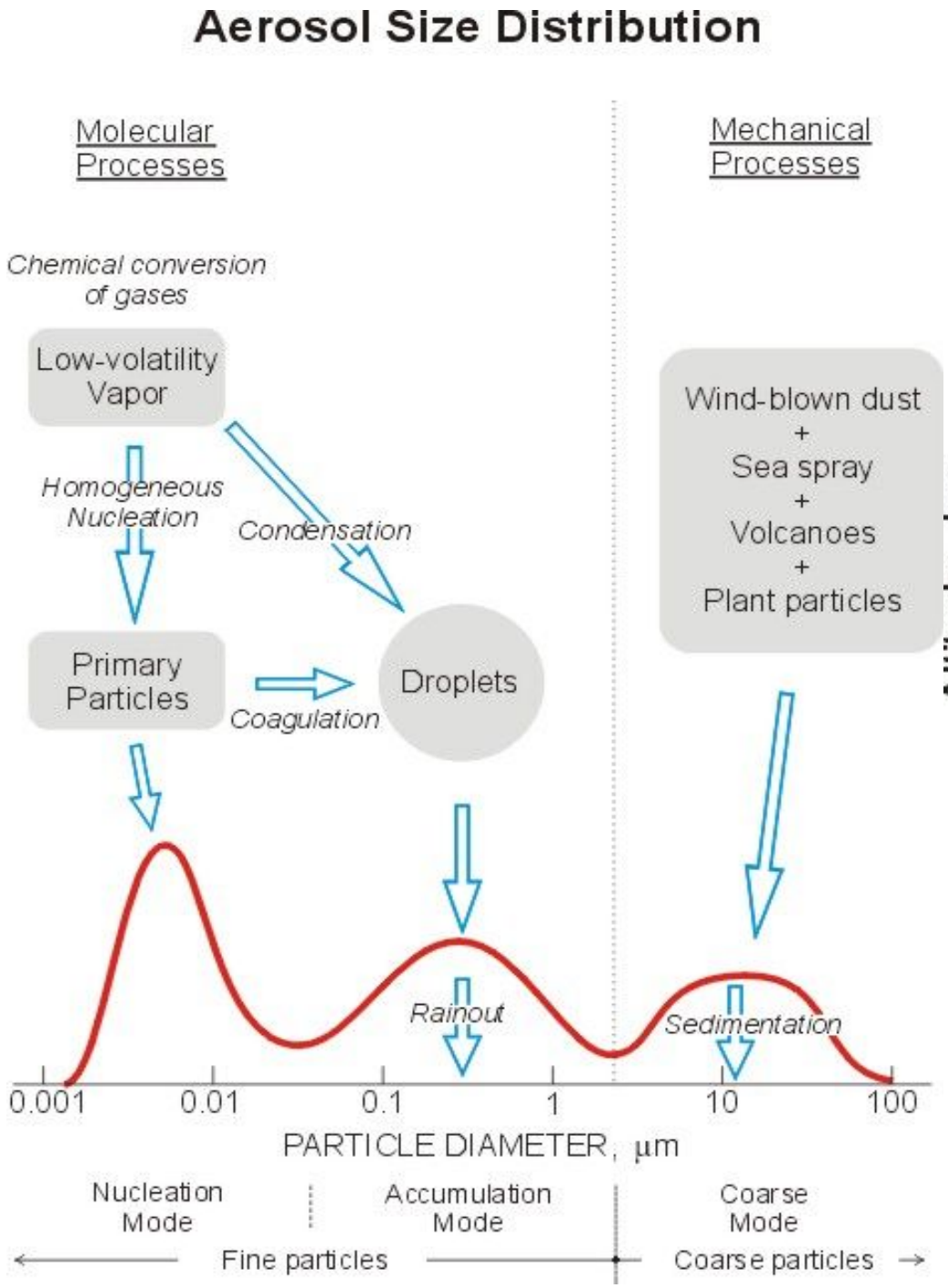

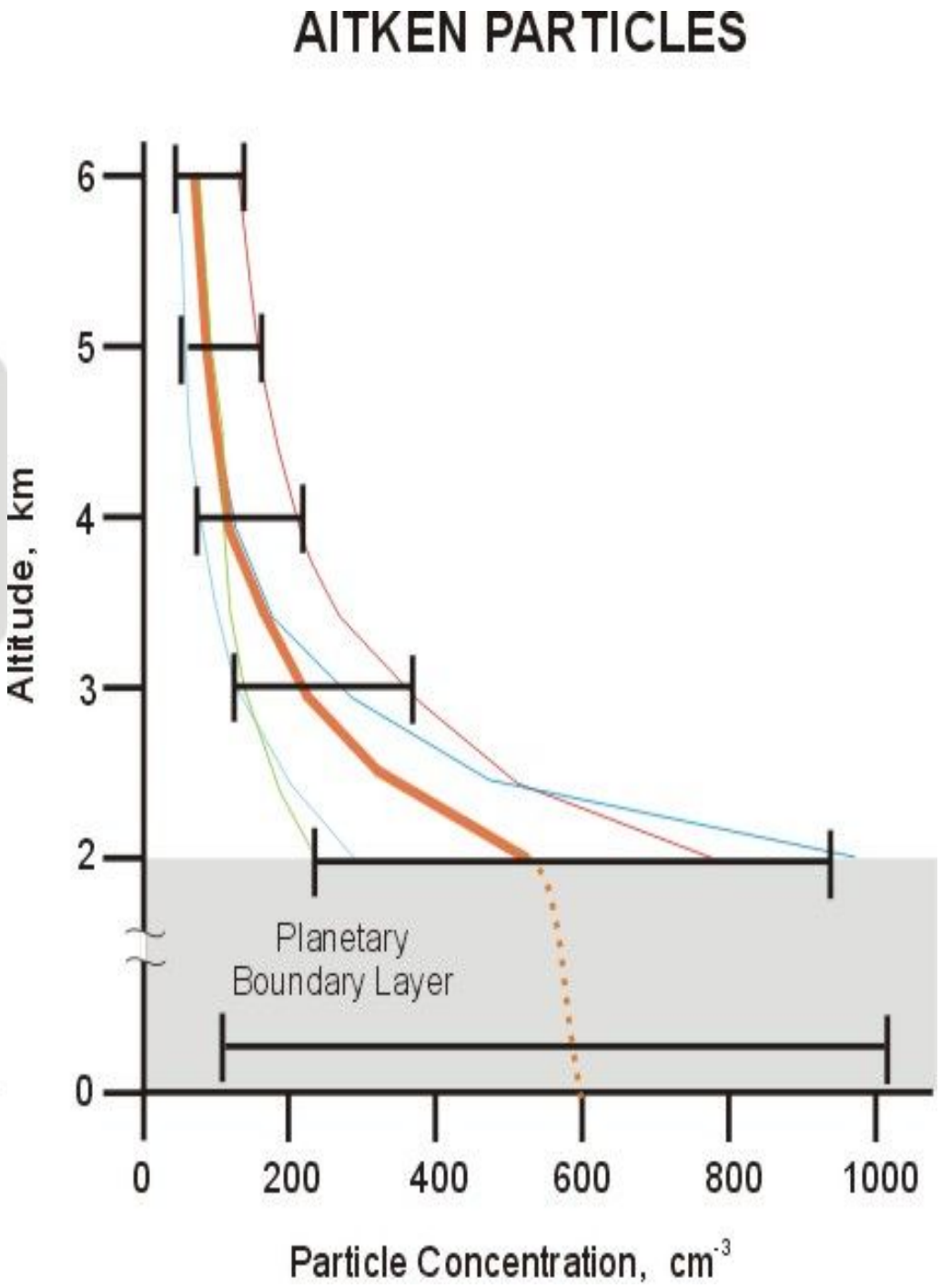

CCN activation:
Kohler theory

$$S = \frac{e}{e_s} \approx 1 + \frac{A}{r} - \frac{B}{r^3} \qquad (2)$$

where $A = \frac{2M_w\sigma_{w/v}}{RT\rho_w}$ and $B = \frac{\nu m_s M_w}{M_s(4/3\pi\rho_w)}$, where ν is the number of dissociated ions per solute molecule, m_s is the the solute mass and subscripts s and w relate to solute and water properties, respectively. The term in A is denoted the Kelvin or curvature term, and that in B, the Raoult or solute term.

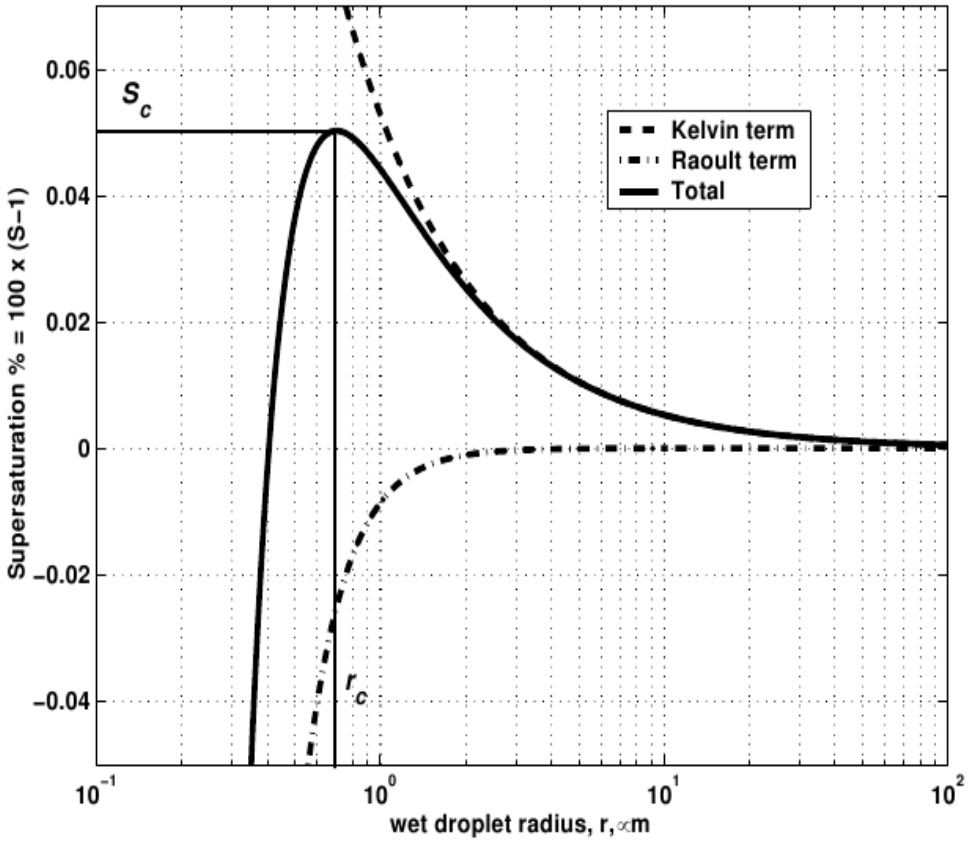

Fig. 1. The Kohler equation can be envisaged as the **competition between the curvature (Kelvin) and solute (Raoult) terms**.

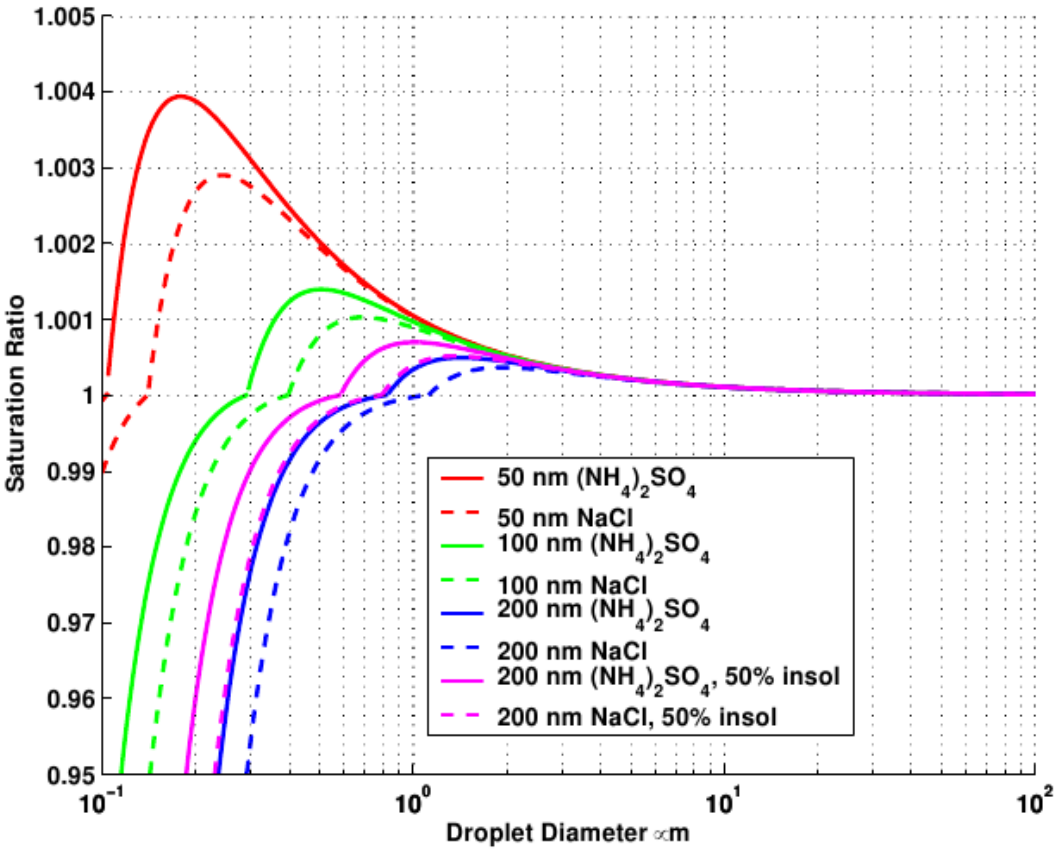

Fig. 3. Activation curves for a range of dry diameter of salt ((NH4)2 SO4 – solid, NaCl – dashed) particles (red, green and blue curves) and for 200 nm particles containing 50% by mass insoluble core (magenta).

McFiggans et al., 2006 www.atmos-chem-phys.net/6/2593/2006/

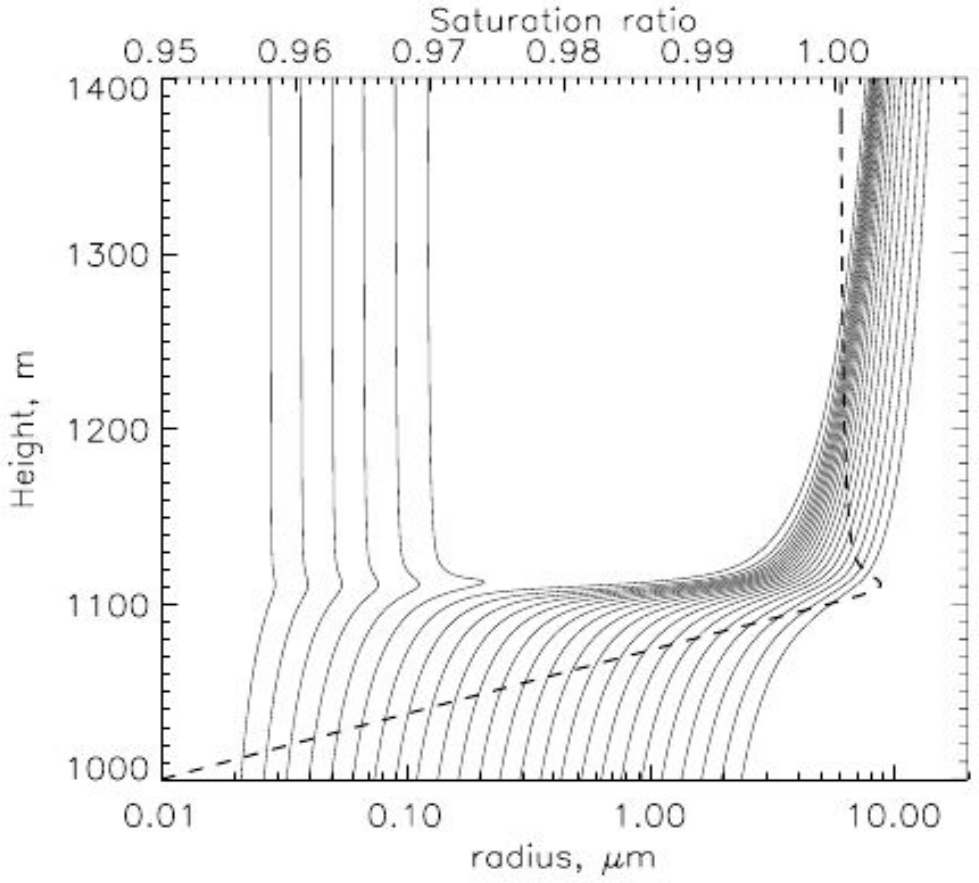

Fig. 4. Simulation showing the change in droplet radius with height in a simulation initialized with an ammonium sulphate aerosol with a geometric mean diameter of 140nm, a geometric standard deviation, σ of 1.7 and aerosol number concentration of 300 cm^{-3} (corresponding to a total mass loading of 0.76μgm^{-3}). The simulation was started at an RH of 95% at 1000 m. Solid lines represent selected aerosol size classes. The dashed line is the saturation ratio.

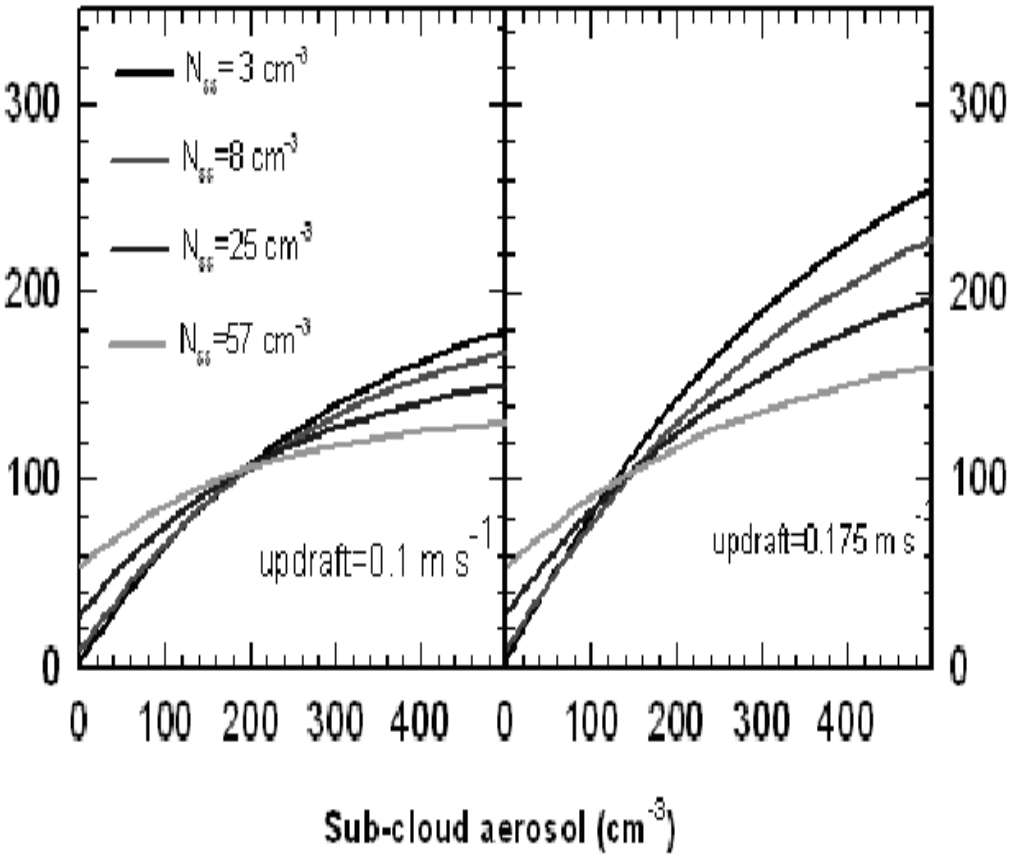

Fig. 5. Cloud droplet concentration as a function of sub-cloud aerosol where the sub-cloud aerosol comprises an external mix of sulphate and sea-salt CCN.

Activation of CCN at cloud base

McFiggans et al., 2006 www.atmos-chem-phys.net/6/2593/2006/

Aerosol, cloud and rain droplets:

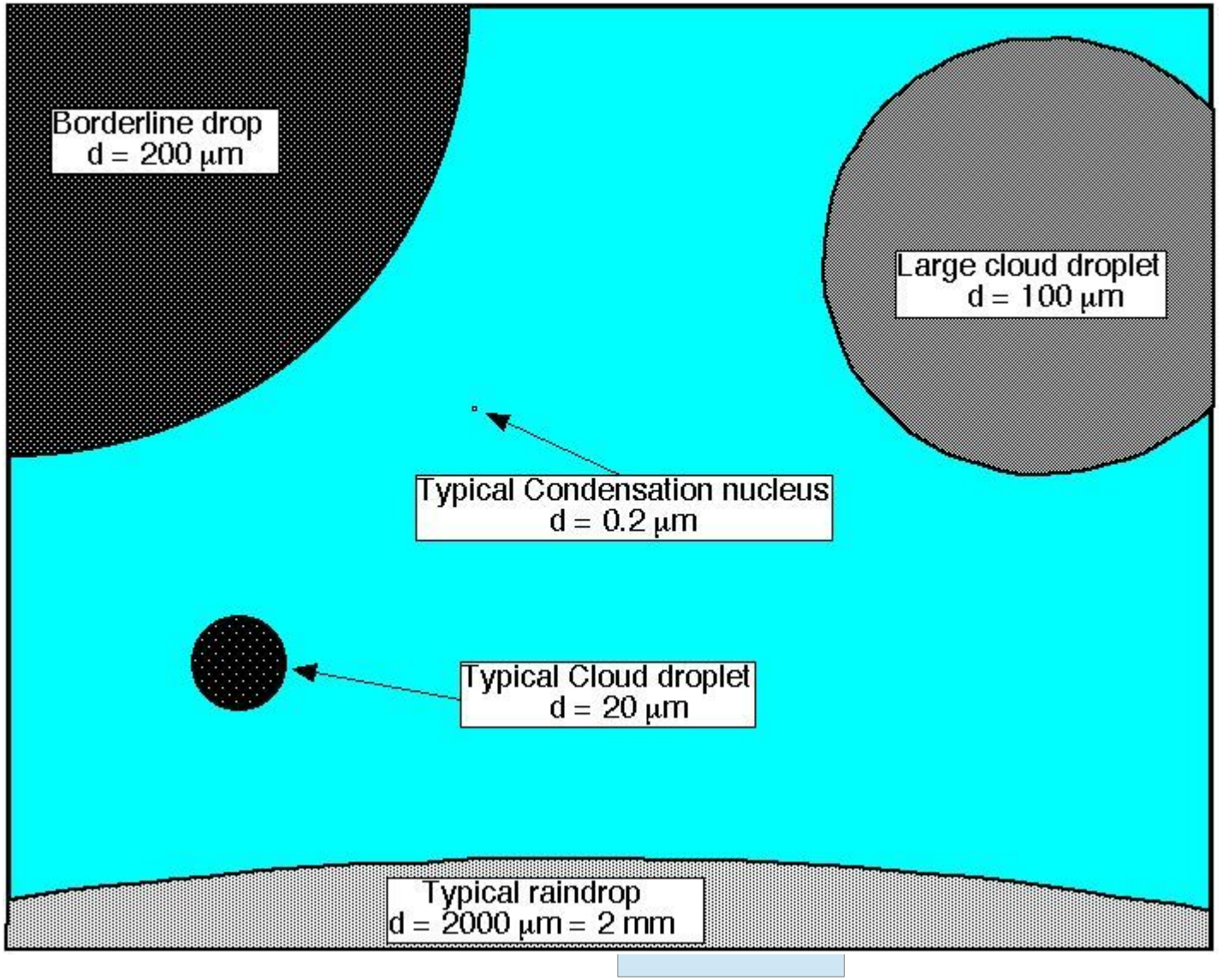

From: What about weather modification? By Chuck Doswell, http://www.flame.org/~cdoswell/wxmod/wxmod.html
After: McDonald, J.E., 1958: The physics of cloud modification. Adv. Geophys., 5, 223-303.

CLOUD-PARTICLE FALLSPEEDS

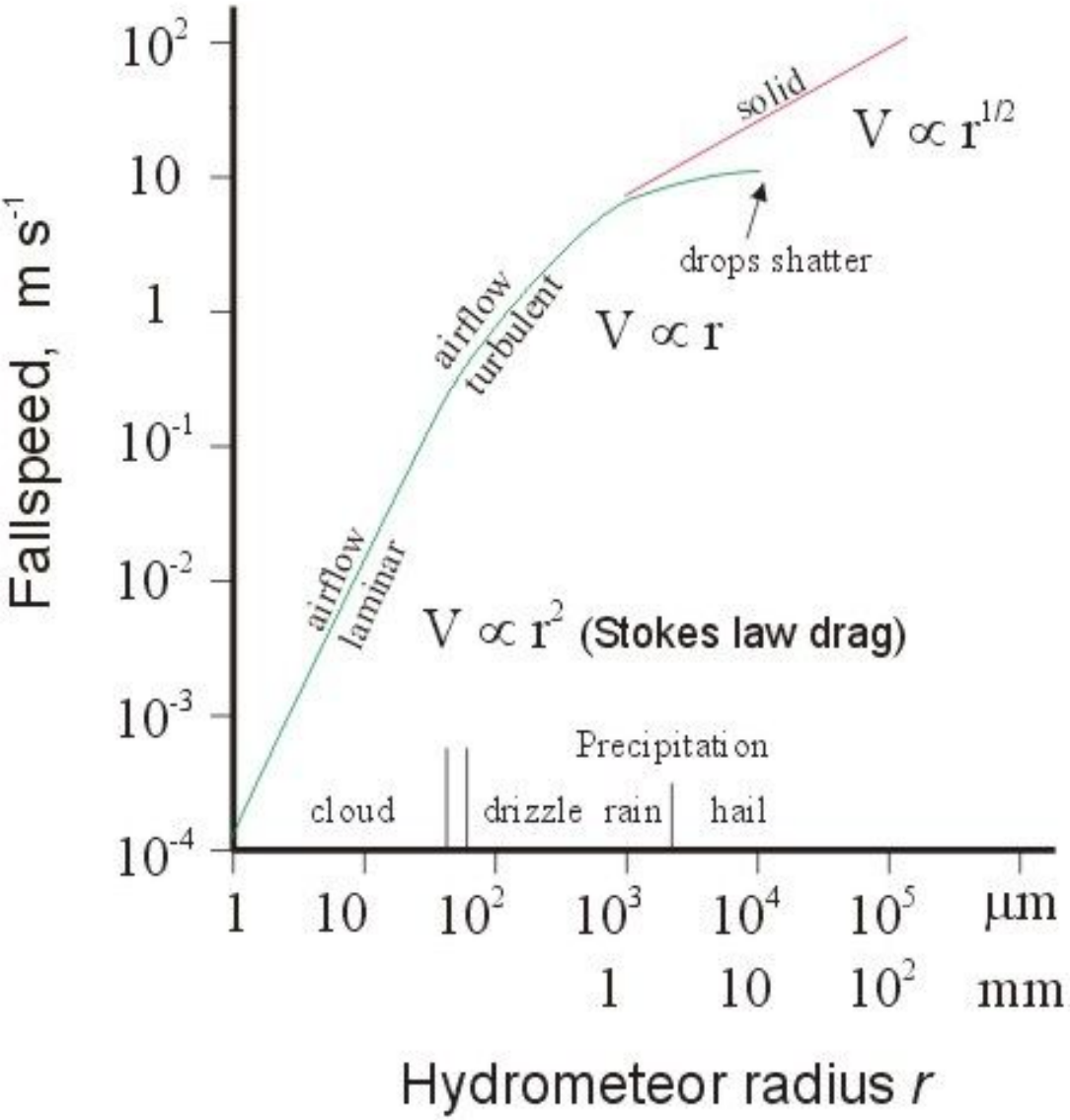

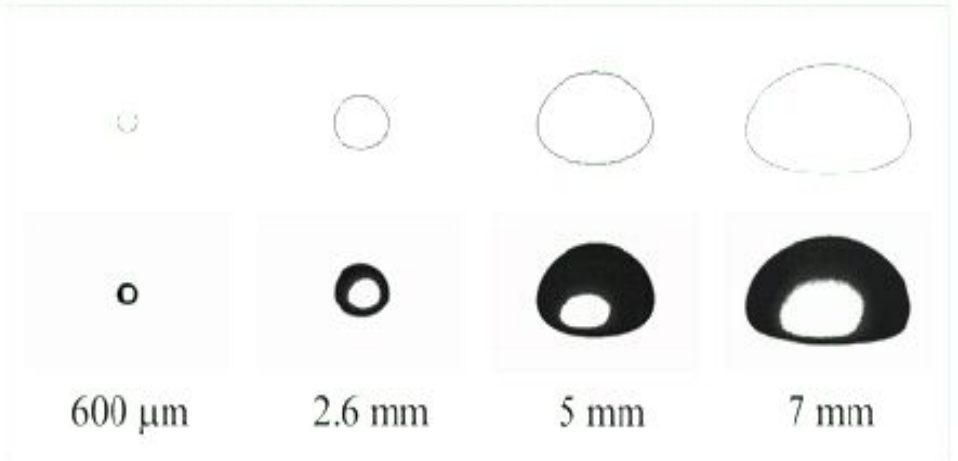

Fig. 1. Calculated drop shapes and real images of drops with different sizes floated in the Mainz vertical wind tunnel

Adapted from McIlveen (1992)

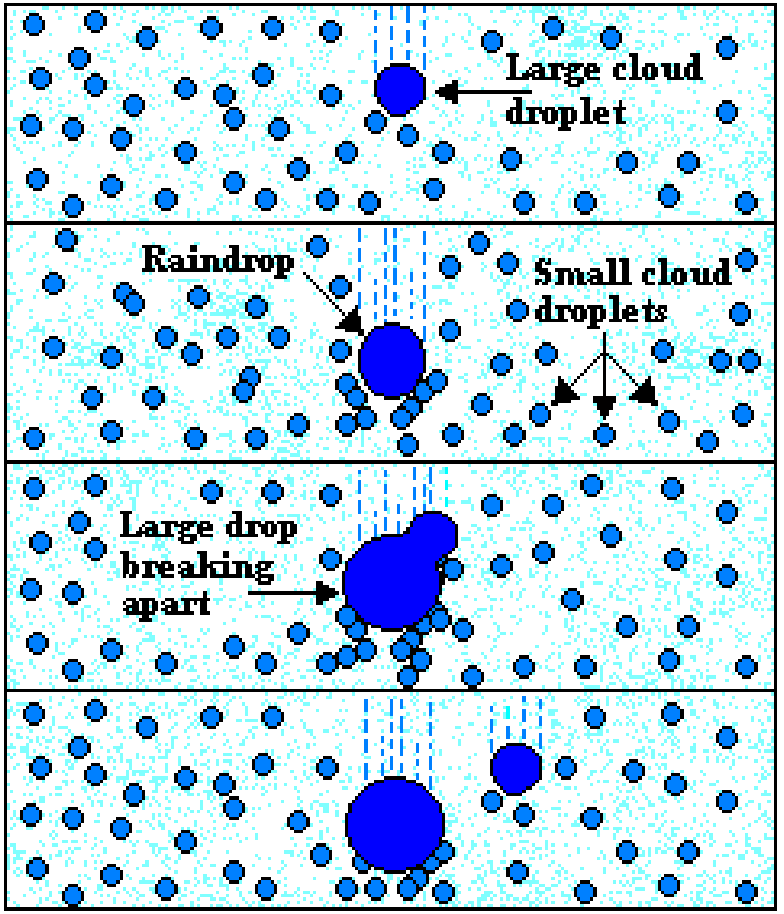

Collision-coalescence process

Mass of typical raindrop is is MILLION times larger than mass of typical cloud droplet.

Such droplets are formed due to collision-coalescence:

substantially different terminal velocities required!

Rain formation

HOW large droplets responsible for collision/coalescence cascade may appear in clouds???

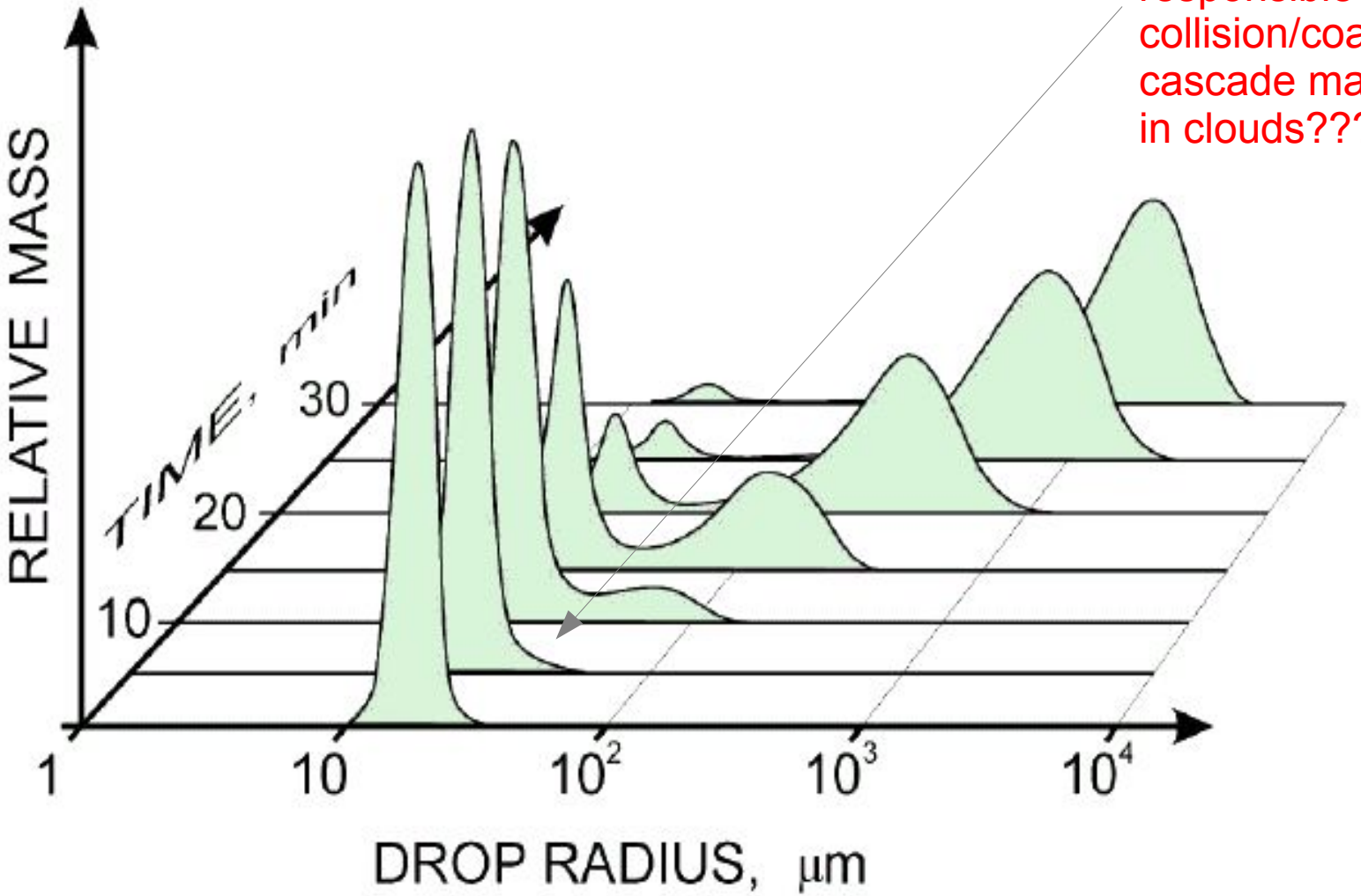

Figure 3 Illustration of the evolution of a droplet size distribution during the onset of the collision-coalescence process. Figure adapted from Berry & Reinhardt (1974) and Lamb (2001), courtesy of D. Lamb, Penn State University.

After Shaw, 2003.

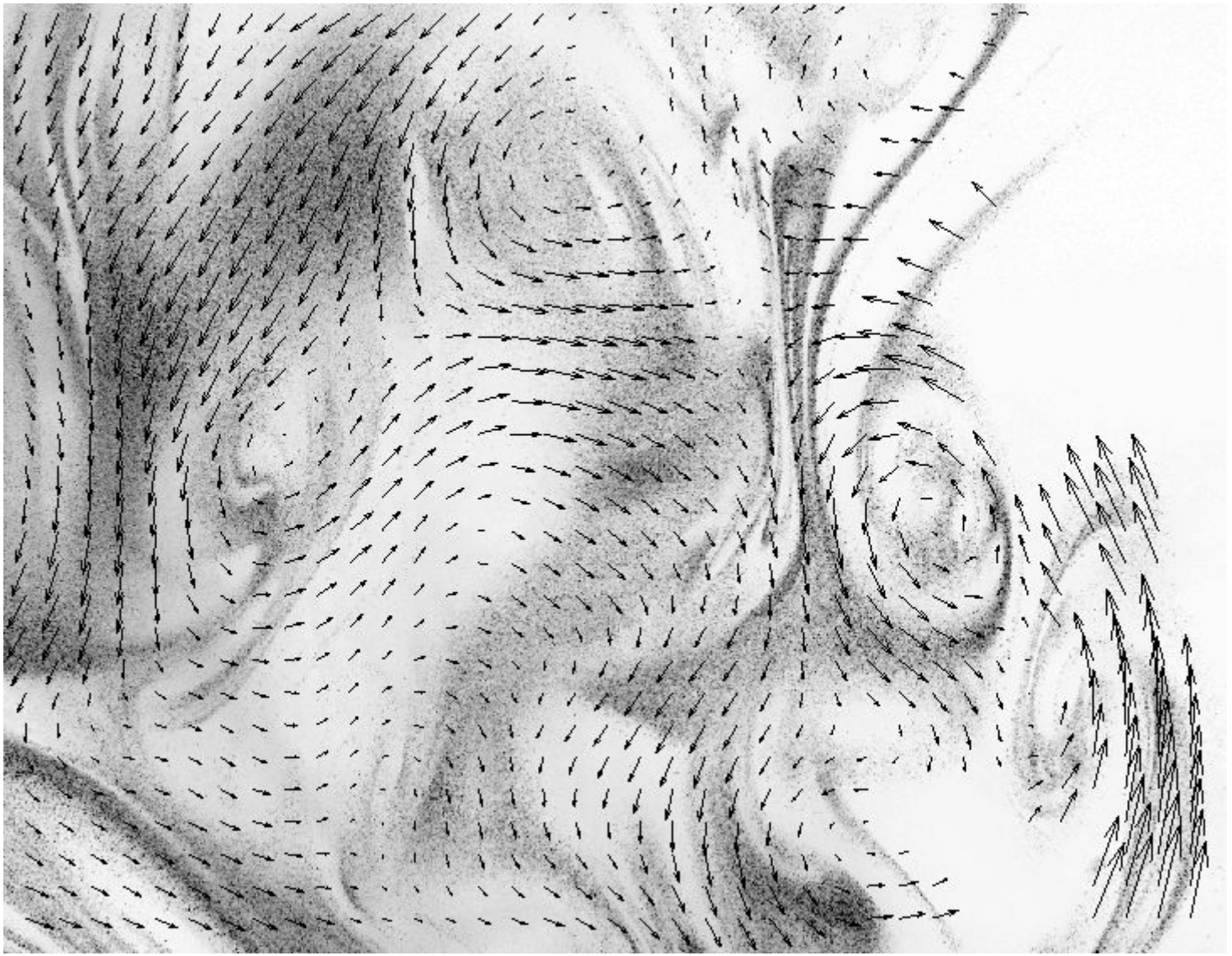

Effects due to turbulent mixing:

preferential concentration,

homogeneous vs. inhomogeneous mixing.

Stokes law, (after Shaw, 2003):

Fundamental to understanding the influence of turbulence on cloud processes is the motion of an individual cloud droplet. In many basic treatments of cloud processes, droplets are assumed to move with a steady-state fall velocity V_T, but this neglects the contribution of fluid accelerations, which under some flow conditions are of the same order or larger than the gravitational acceleration g. For small cloud droplets, the Reynolds number typically is sufficiently small so that the Stokes drag force is a reasonable approximation. In this limit, Newton's second law for a sphere with velocity $\mathbf{v}$ in a viscous fluid with uniform (but time varying) velocity $\mathbf{u}$ is:

$$\rho_d V_d \frac{d\mathbf{v}}{dt} = 6\pi\mu r\,(\mathbf{u}-\mathbf{v}) + \frac{1}{2}\rho_f V_d\,(\dot{\mathbf{u}}-\dot{\mathbf{v}}) + 6r^2\sqrt{\pi\rho_f\mu}\int_0^t \frac{\dot{\mathbf{u}}(t')-\dot{\mathbf{v}}(t')}{\sqrt{t-t'}}dt'$$
$$+ \rho_d V_d \mathbf{g} + \rho_f V_d\,(\dot{\mathbf{u}}-\mathbf{g})\,. \qquad (11)$$

Here, μ and ρ_f are the dynamic viscosity and density of the surrounding fluid (air), ρ_d is the density of the droplet (water), and $V_d = 4/3\pi r^3$ is the droplet volume. The terms on the right are, in order, the Stokes drag force, the "added mass" force due to acceleration of the surrounding fluid, the Basset "history" force due to diffusion of vorticity from an accelerating particle, the gravitational force, and finally, two terms resulting from the stress field of the fluid flow acting on the particle (including a shear stress term and a pressure gradient or buoyancy term).

Lagrangian accelerations are dominant at the smallest spatial scales of the flow, corresponding to the dissipation or Kolmogorov scale λ_k . Because it is assumed that properties of the dissipation scale eddies depend only on v and it follows that these eddies will have a timescale $\tau_k = (v/\varepsilon)^{1/2}$, where ε is the TKE dissipation rate.

Therefore the Stokes number for droplets in a turbulent flow is:

$$S_d = \frac{\tau_d}{\tau_k} = \frac{2\rho_d \epsilon^{1/2} r^2}{9\rho_f \nu^{3/2}}.$$

For typical cloud conditions ($\varepsilon \sim 10^{-2}$ m^2 s^{-3} , $v \sim 10^{-5}$ m^2 s^{-3}) and $r \sim 10^{-5}$ m, the Stokes number is close to the order $S_d \sim 10^{-1}$.

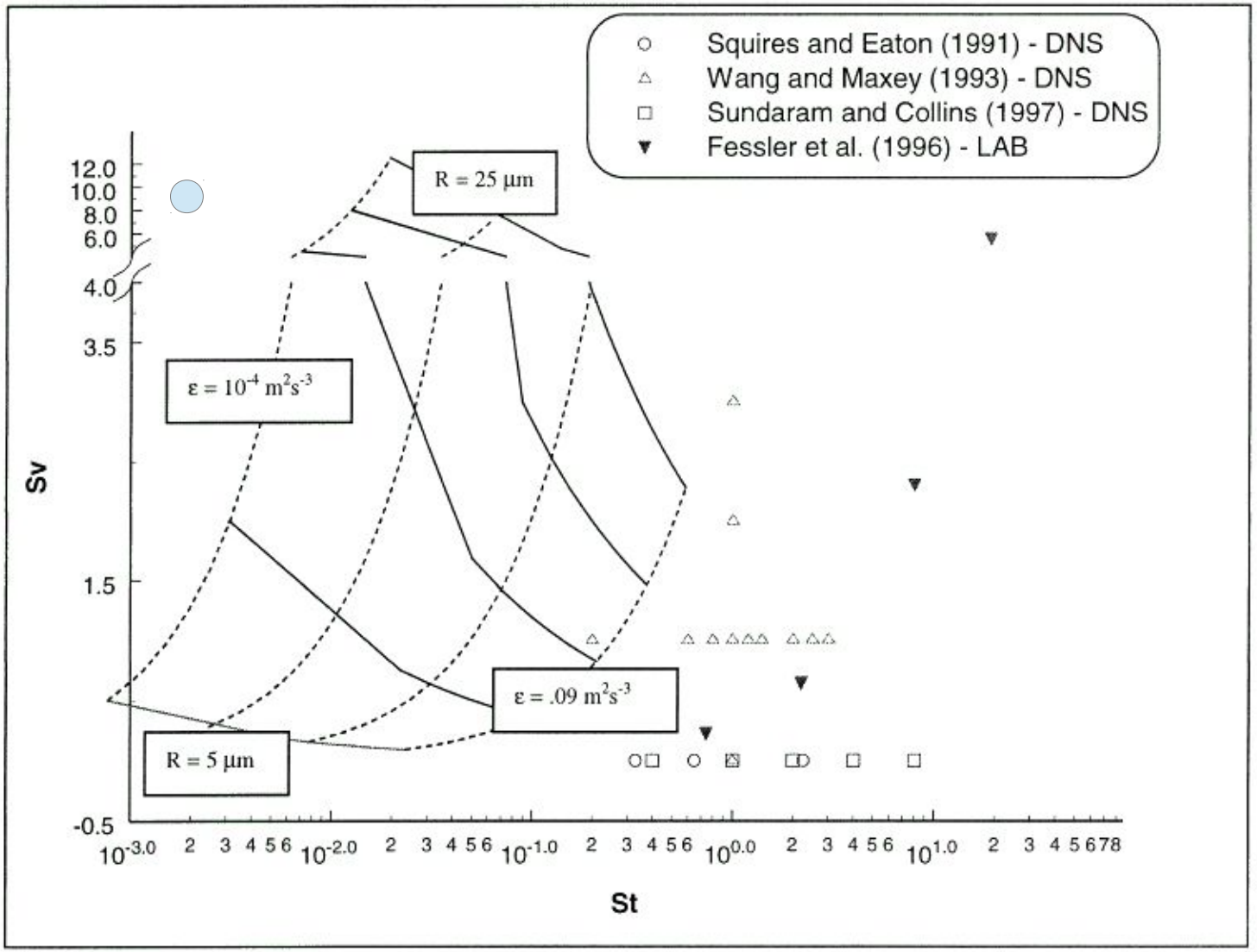

FIG. 1. Stokes number (S_t)–velocity ratio (S_v) diagram showing location of direct numerical simulations (DNS) and laboratory experiments (LAB) for particles in 3D turbulence. The S_t–S_v region for cloud droplets of 5–25-μm radius is shown for an appropriate range of eddy dissipation rates (10^{-4}–0.09 m^2 s^{-3}). The dashed lines are for constant eddy dissipation rates (10^{-4}, 10^{-3}, 10^{-2}, and 0.09 m^2 s^{-3}) and radii varying from 5 to 25 μm, while the solid lines are for constant radii (5, 10, 15, 20, and 25 μm).

Vaillancourt and Yau, 2000.

The Stokes number St is the ratio between the particle's response time and a characteristic timescale of the flow.

The velocity ratio Sv is the ratio of the eddy turnover time of that eddy and the time it takes for the particle to sediment across the eddy.

TABLE 1. Characteristic Kolmogorov scales for eddy dissipation rates observed in cumulus clouds.

Energy dissipation rate ε ($m^2 s^{-3}$)	Kolmogorov length η (cm)	Kolmogorov time τ_η (s)	Kolmogorov velocity v_η (cm s^{-1})
1×10^{-5}	0.45	1.25	0.35
1×10^{-4}	0.25	0.4	0.63
1×10^{-3}	0.14	0.13	1.1
0.01	0.08	0.04	2.0
0.1	0.045	0.01	3.5

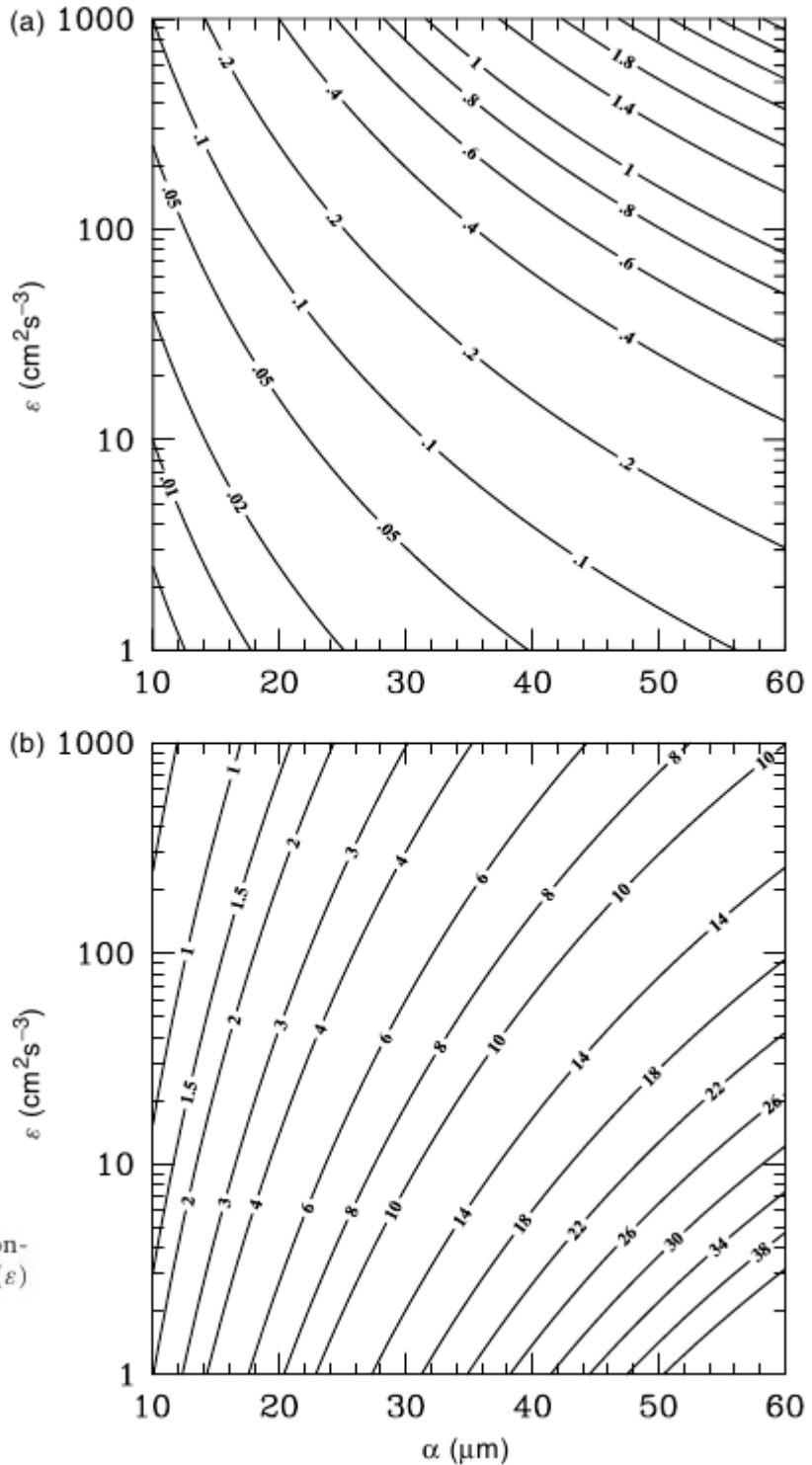

Figure 1. Contour plots of (a) Stokes number (St) and (b) non-dimensional terminal velocity (Sv) as a function of flow dissipation rate (ε) and droplet radius (a) (Ayala *et al.*, 2008a).

St=0.001
and less

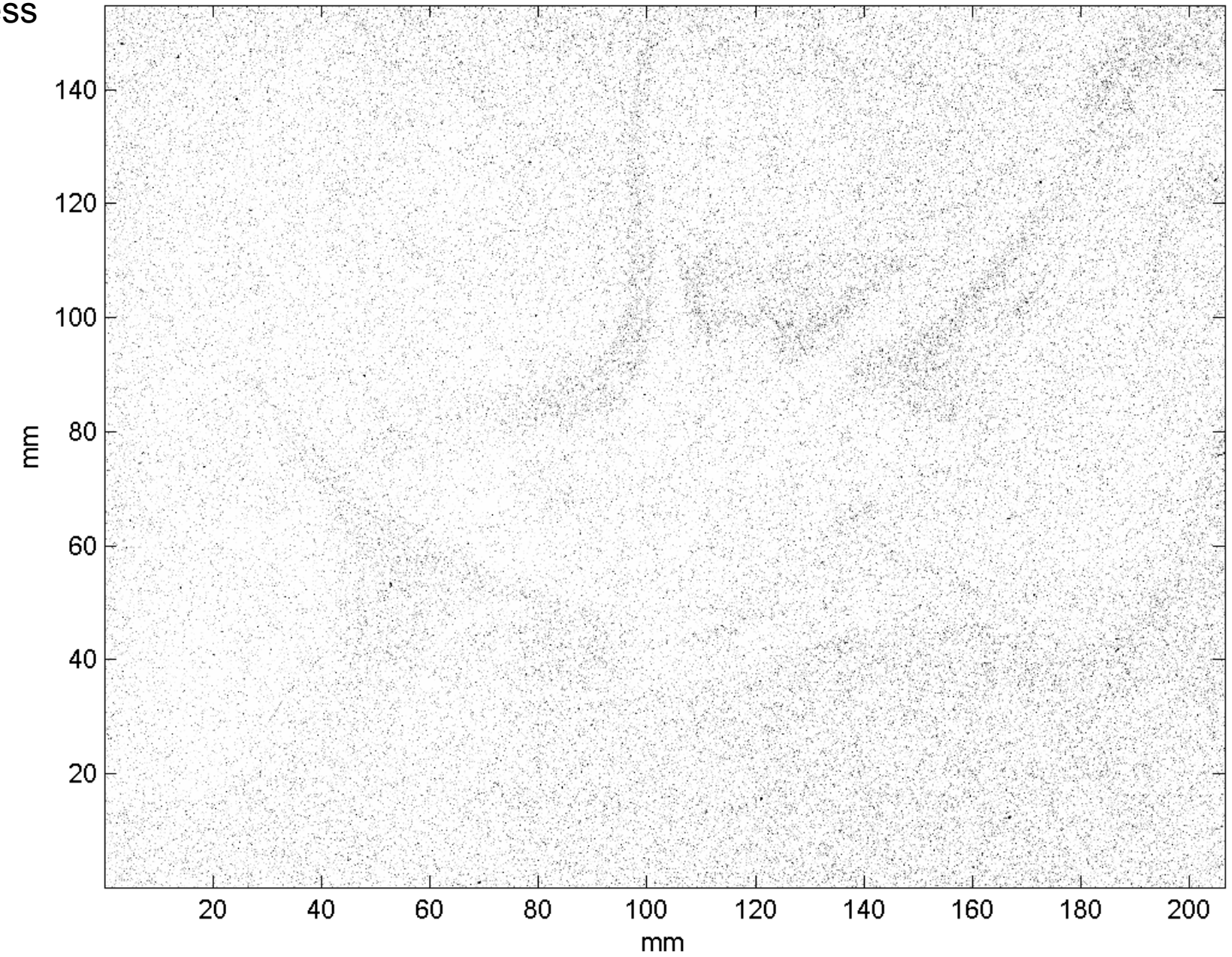

Jaczewski and Malinowski, 2005

No mixing.

$\varepsilon = 6 \times 10^{-5}\,\mathrm{m^2 s^{-3}}$

TABLE 1. MEAN DROPLET CONCENTRATIONS AND LOCAL DROPLET CONCENTRATIONS AT SCALES OF 4 AND 80 MM

Image number	Local droplet concentration at 4 mm scale (mm^{-2})	Mean droplet concentration (mm^{-2})	Local droplet concentration at 80 mm scale (mm^{-2})	$D - E$
Test	7.2	7.2	7.2	0.0001
1	7.5	7.1	6.8	−0.0346
2	9.1	8.7	8.6	−0.0236
3	9.4	9.0	8.8	−0.0245
4	8.9	8.6	8.5	−0.0150
5	9.7	9.4	9.5	−0.0093
6	7.7	7.3	7.2	−0.0193
7	9.3	9.1	9.0	−0.0122
8	6.3	6.2	6.1	−0.0080
9	5.4	5.3	5.2	−0.0108
10	5.5	5.3	5.2	−0.0169

Values are calculated according to (6) and the values of $D - E$ for the test image and for ten experimental images, where D is the correlation dimension and E is the Euclidean dimension. See text for details.

$$\langle C \rangle_r = \frac{\langle N \rangle_r}{\pi r^2},$$

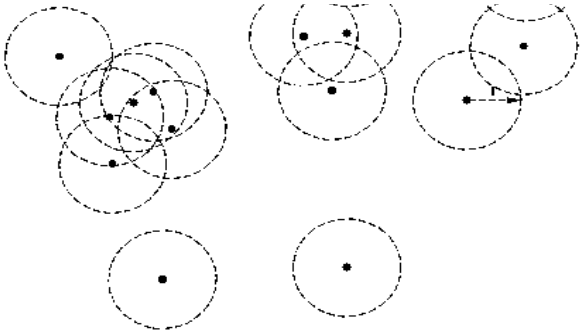

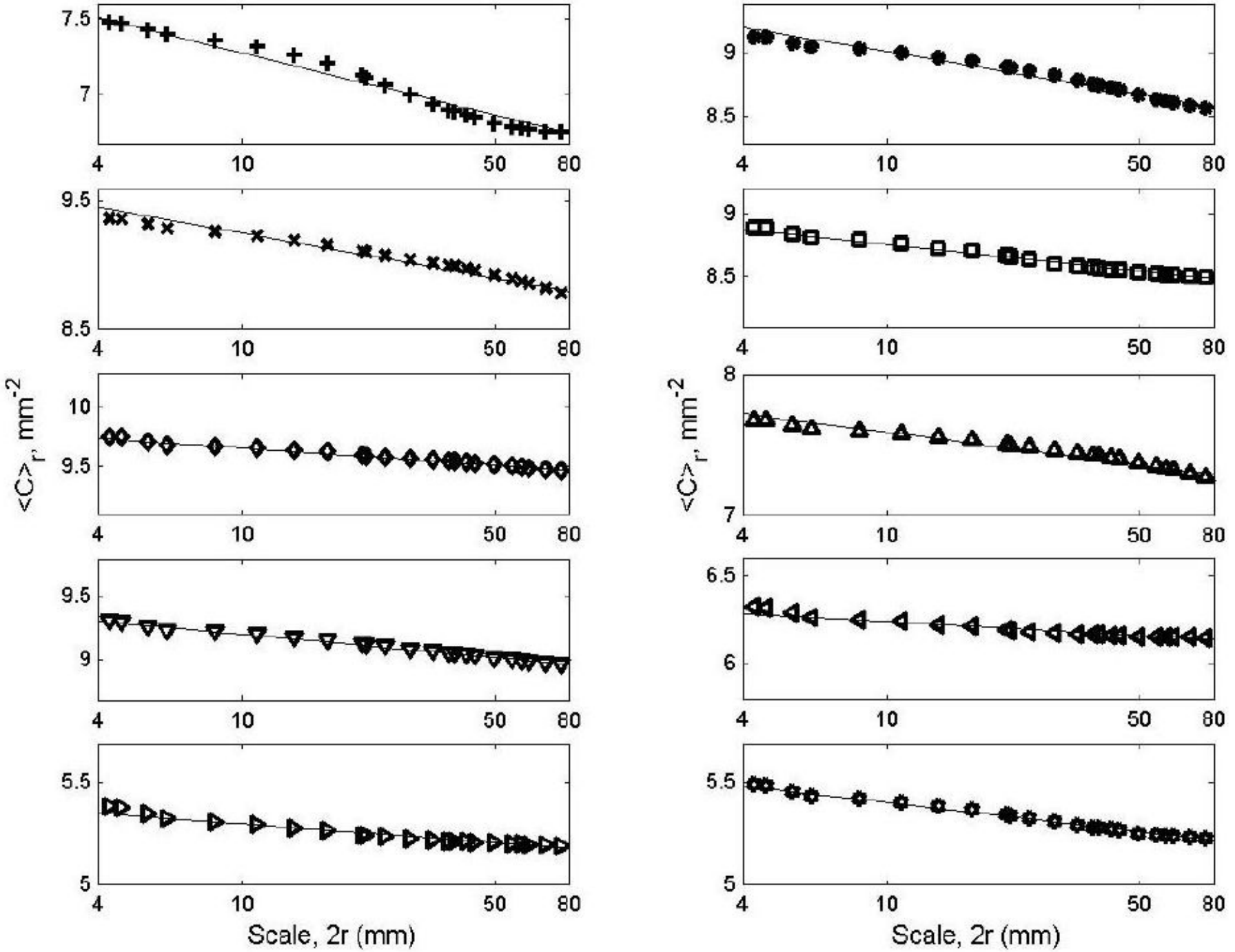

Figure 7. The dependence, calculated according to (7), of the local droplet concentration $\langle C \rangle_r$ on scale for each of the ten experimental images. See text for details.

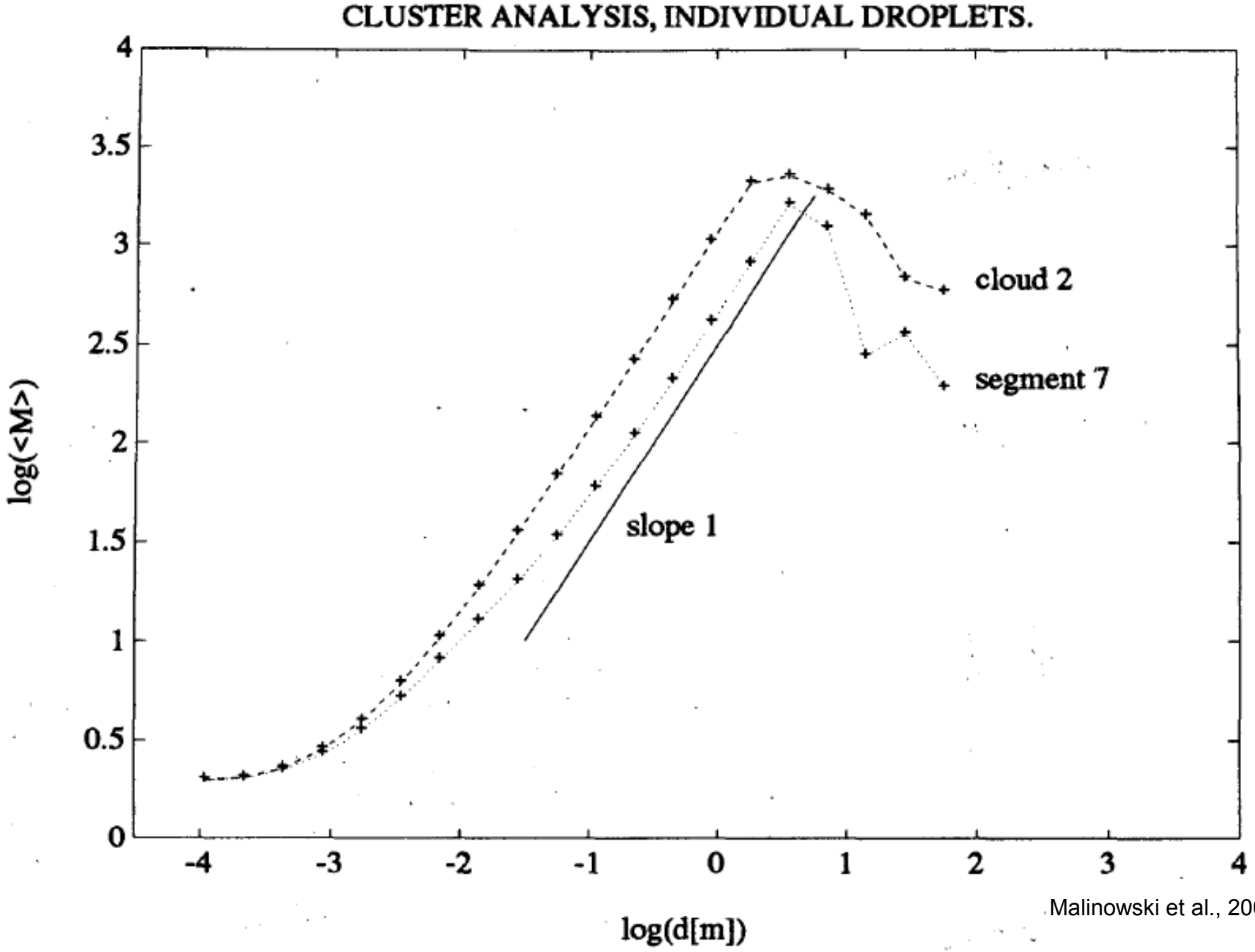

Malinowski et al., 2004

FIG. 4. Results of cluster analysis of positions of individual droplets. Cloud 2 (solid line) and segment 7 (dashed line).

Collisions, coalescence and turbulence

The collision and coalescence of droplets in a turbulent flow are governed by
(i) geometric collisions due to droplet-turbulence interactions;
(ii) collision efficiency due to droplet-droplet interactions and
(iii) coalescence efficiency due to droplet surface properties.

In practice, it is difficult to distinguish between collision and coalescence and the experimentally measurable quantity is collection efficiency defined as the ratio of the actual cross-section for droplet coalescence to the geometric cross-section.

Geometric collisions
DNS results (e.g. Franklin et al. 2007; Ayala et al. 2008a) show that **turbulence can increase the collision kernel relative to the case of stagnant air by two effects:**

droplet relative velocity

droplet clustering.

Turbulence may also affect the droplet relative velocity through preferential sweeping whereby droplets bias their downward trajectories towards regions of higher turbulence thus increasing their terminal velocities relative to still air.

Caustics (sling effect) are also considered (e.g. Falkovich and Pumir, 2007)

In multidisperse suspensions, $|w_{12}|$ is always larger than its monodisperse counterpart.

This can be understood by considering a limiting case of monodisperse suspension, in the absence of gravity. For low St, velocities of equally sized droplets are strongly correlated, both with the fluid and each other.

As St increases, the correlation of the droplets with the flow and each other decreases and $|w_{12}|$ increases.

However, for St>>1, droplets respond slowly to changes in the fluid velocity and $|w_{12}|$ decreases.

For multidisperse droplets, the velocities of the droplets decorrelate more rapidly than the equivalent monodisperse cases since the droplets with different inertia respond differently to changes in the flow.

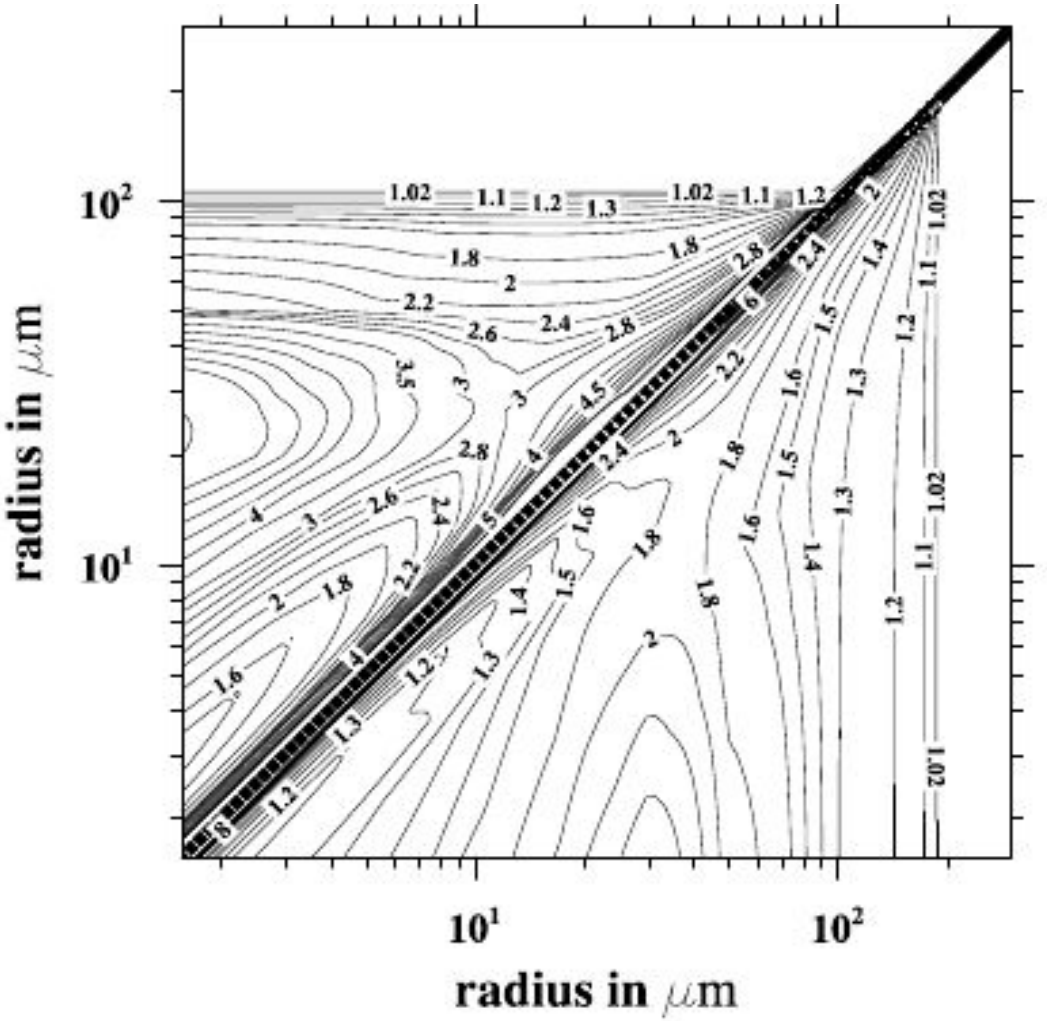

Figure 2. The ratio of a typical turbulent collision kernel to a purely gravitational collision kernel (Grabowski and Wang, 2009). The ratio on the 45^o degree line is undefined due to the zero value of the gravitational kernel. The ratio is essentially one when droplets are greater than 100 μm. The flow dissipation rates are 400 cm^2 s^{-3} and 100 cm^2 s^{-3} in the upper-left and lower-right part of the figure respectively.

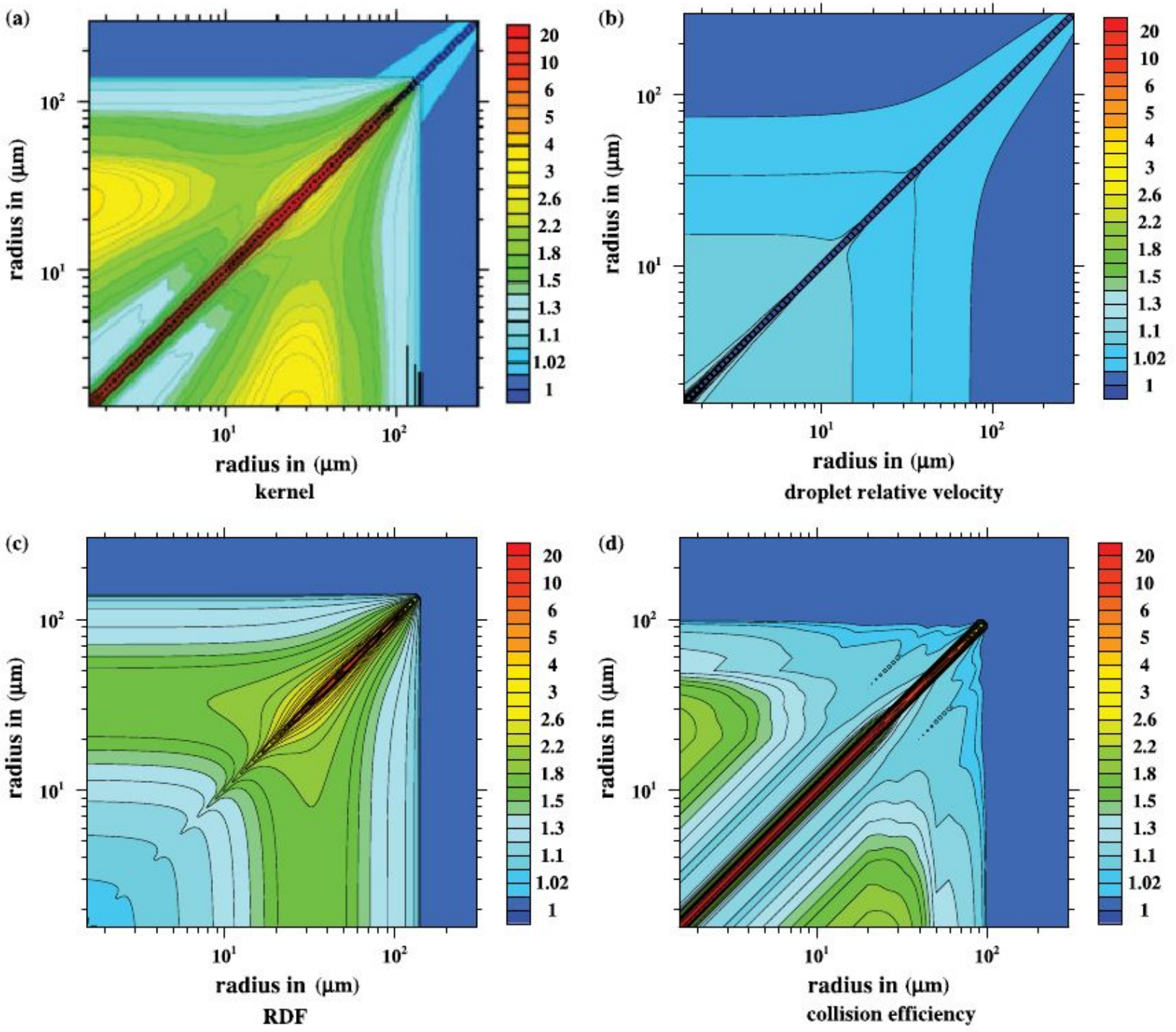

Figure 2. (a) The ratio of a typical turbulent collision kernel to a purely gravitational collision kernel (Wang and Grabowski, 2009) for $\varepsilon = 200$ cm^2 s^{-3}. The ratio on the 45° degree line is undefined owing to the zero value of the gravitational kernel. The ratio is essentially one when droplets are greater than 100 μm. The constituent parts of the turbulent collision kernel are shown in (b) the droplet relative velocity, (c) the RDF and (d) the collision efficiency.

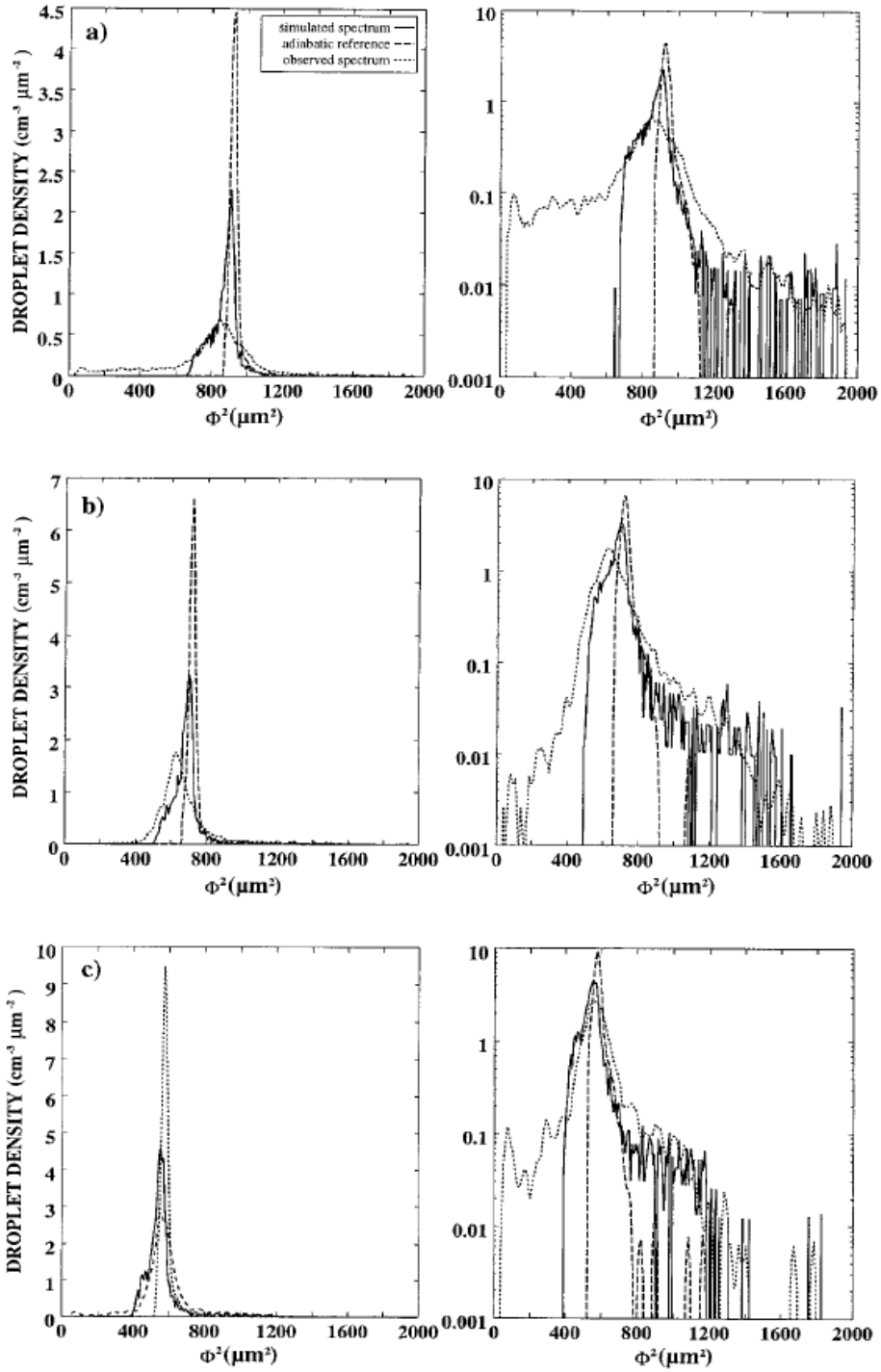

FIG. 4. Three examples of the comparison between an observed spectrum (dotted line) and the adiabatic reference (dashed line), after instrumental broadening by the Fast-FSSP simulator (solid line). The total droplet number concentrations are, respectively, 225 (a), 329 (b), and 455 cm^{-3} (c).

However.....in situ measuremets...

With the **improved** size and spatial resolutions of the Fast-FSSP measurements it has been possible to identify **very narrow spectra** in most of the cloud traverses ...

These spectra are **much narrower than previously measured with the standard probe**.
The regions of narrow spectra show characteristics close to the adiabatic reference, such as LWC values slightly lower than the adiabatic value at that level and values of droplet concentration close to the maximum value within the cloud traverse. **The spectra observed in these regions are narrow but still broader than the adiabatic reference**.
The high concentration densities of droplets with diameter smaller than the mode can be attributed to partial evaporation of some droplets resulting from the mixing with dry air. The occurrence of this process is attested by the slightly subadiabatic values of LWC.

Chaumat and Brenguier, 2001

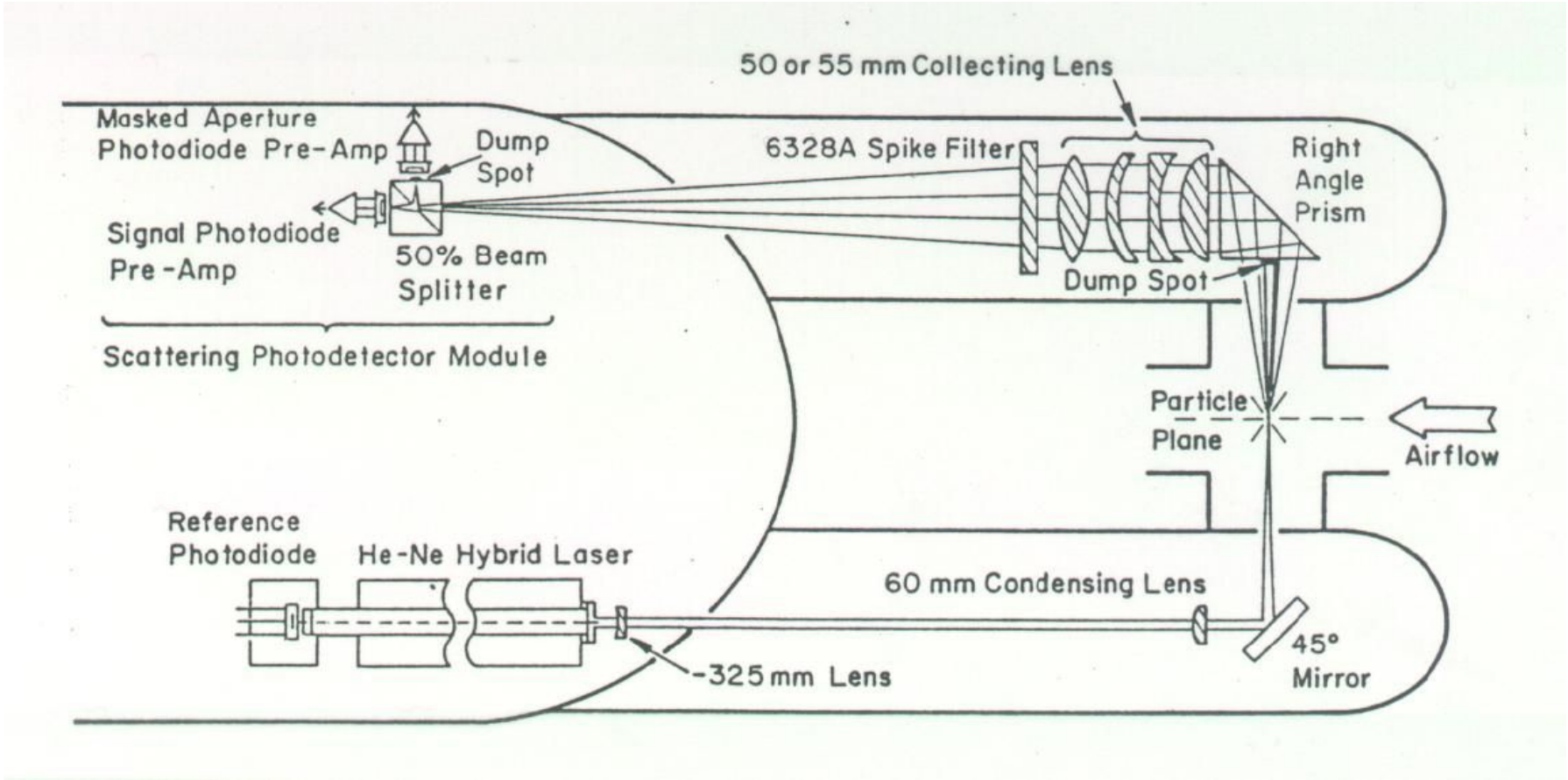
50 or 55 mm Collecting Lens
Masked Aperture
Photodiode Pre-Amp
Dump
Spot
6328A Spike Filter
Right
Angle
Prism
Signal Photodiode
Pre-Amp
50% Beam
Splitter
Dump Spot
Scattering Photodetector Module
Particle
Plane
Airflow
Reference
Photodiode
He-Ne Hybrid Laser
60 mm Condensing Lens
45°
Mirror
-325 mm Lens

Geometrical considerations: droplets in the prescribed flow

- vortex of horizontal axis, stretched...

Simplified Stokes eq.:

$$m\frac{d\mathbf{V}}{dt} = -6\pi R\mu(\mathbf{V}-\mathbf{u}) + m\mathbf{g}, \qquad (1)$$

where μ is the viscosity of the air, $\mathbf{g}$ is gravitational acceleration and $\mathbf{u}$ is a the air flow field in the cloud which for the sake of this problem we assume to be prescribed, i.e. unaffected by the droplets. Although droplets are passively carried by the air they are not passive tracers, as the trajectories they trace out are different from the paths of the fluid elements.

Let (r, θ, z) be polar co-ordinates with the Oz direction along the vortex axis inclined at an angle ϕ from the vertical. In this frame of reference the gravity force takes the form

$$\mathbf{g} = g\sin\phi\cos\theta\hat{\mathbf{e}}_r - g\sin\phi\sin\theta\hat{\mathbf{e}}_\theta - g\cos\phi\hat{\mathbf{e}}_z. \qquad (2)$$

The velocity field $\mathbf{u}$ is a sum of the flow due to the uniform irrotational straining flow, and the flow due to an axisymetric vortex having azimuthal velocity $u(r)$,

$$\mathbf{u} = -\tfrac{1}{2}\alpha r\hat{\mathbf{e}}_r + \alpha z\hat{\mathbf{e}}_z + u(r)\hat{\mathbf{e}}_\theta. \qquad (3)$$

Bajer et al., 2000

The equation (1) takes the form

$$\tau_d \left(\frac{dV_r}{dt} - \frac{V_\theta^2}{r} \right) = - \left(V_r + \tfrac{1}{2}\alpha r \right) + V_g \sin\phi \cos\theta, \quad (4)$$

$$\tau_d \left(\frac{dV_\theta}{dt} + \frac{V_\theta V_r}{r} \right) = - \left(V_\theta - u(r) \right) - V_g \sin\phi \sin\theta, \quad (5)$$

$$\tau_d \frac{dV_z}{dt} = - \left(V_z - \alpha z \right) - V_g \cos\phi, \quad (6)$$

where $\tau_d = m/(6\pi R\mu)$ is the characteristic time of the droplet response to the changes in fluid velocity and $V_g = g\tau_d$ is the terminal velocity of the gravitational settling.

In the following we will consider a model vortex with total circulation Γ and gaussian distribution of vorticity. The azimuthal velociy $u(r)$ is given by

$$u(r) = \frac{\Gamma}{2\pi r}\left(1 - \mathrm{e}^{-(r/2\delta)^2}\right), \quad \delta = N\sqrt{\nu/\alpha}. \quad (7)$$

Here the dimensionless number N is the ratio of the vortex radius δ and the radius of the familiar Burgers vortex, an exact steady solution of the Navier-Stokes equation likely to be a good model of the small-scale coherent structures in turbulence.

In the Stokes regime (1) droplets of radius R adapt their speed to that of ambient flow on the time-scale

$$\tau_d = (2\rho_w R^2)/(9\mu), \tag{8}$$

where ρ_w is the density of water and μ is the viscosity of air and the corresponding length scale is equal

$$S = \sqrt{\Gamma\tau_d/2\pi}. \tag{9}$$

The motion along the vortex axis separates and in dimensionless units equations (4-5) governing the motion in the vertical plane take form

$$\ddot{r} - r\dot{\theta}^2 = -\tfrac{1}{2}L_1 r - \dot{r} - L_2 \sin\theta, \tag{10}$$

$$2\dot{r}\dot{\theta} + r\ddot{\theta} = r^{-1} - r\dot{\theta} - L_2 \cos\theta, \tag{11}$$

where

$$L_1 = \alpha\tau_d, \quad L_2 = g\tau_d^2(2\pi/\Gamma\tau_d)^{1/2} \tag{12}$$

are two non-dimensional numbers characterising the droplet.

Equations (10-11) have one stable fixed point when $L_1 < L_2^2$ and one limit cycle otherwise. Small droplets tend to the limit cycle and keep circulating around the vortex axis. Large droplets move towards the fixed point (figure 1).

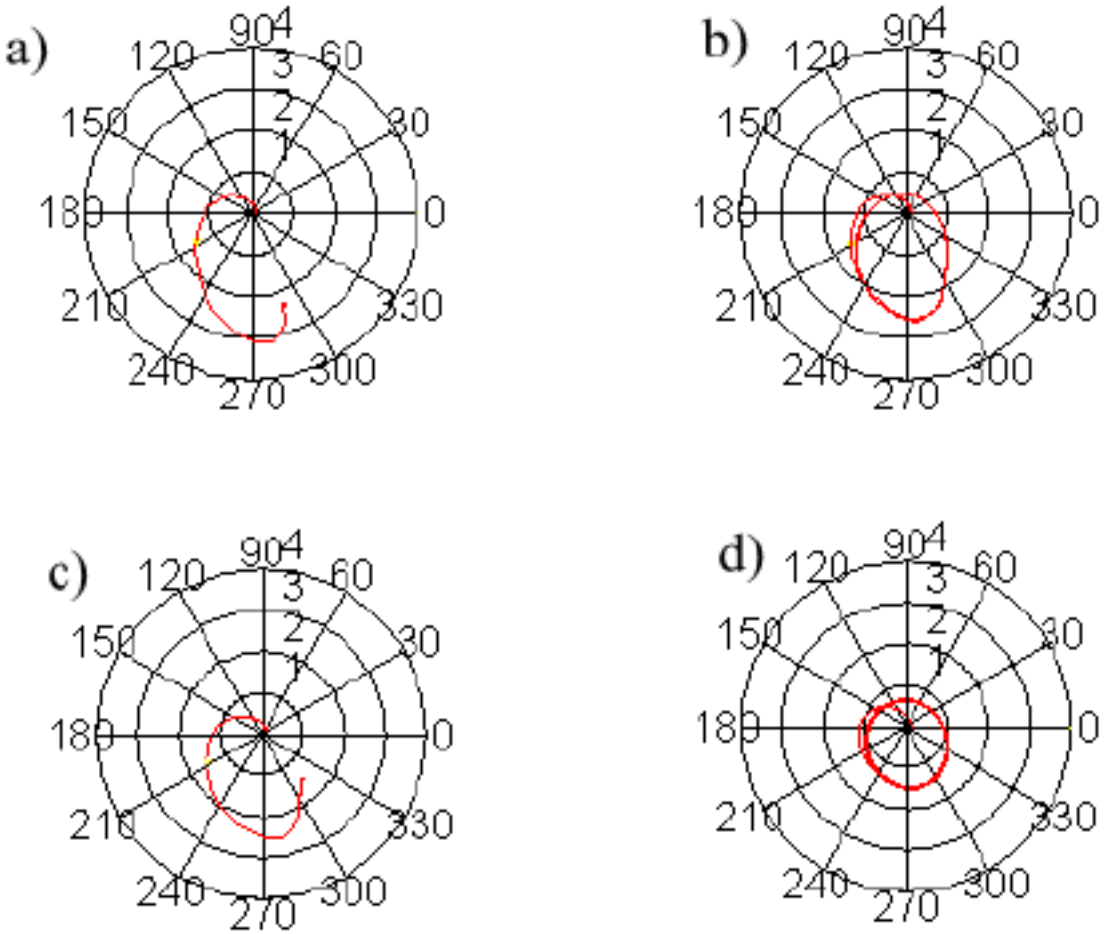

Figure 1: The trajectories of droplets with L_1 / L_2^2 equal a) 0.8; b) 1.004; c) 1; d) 2.

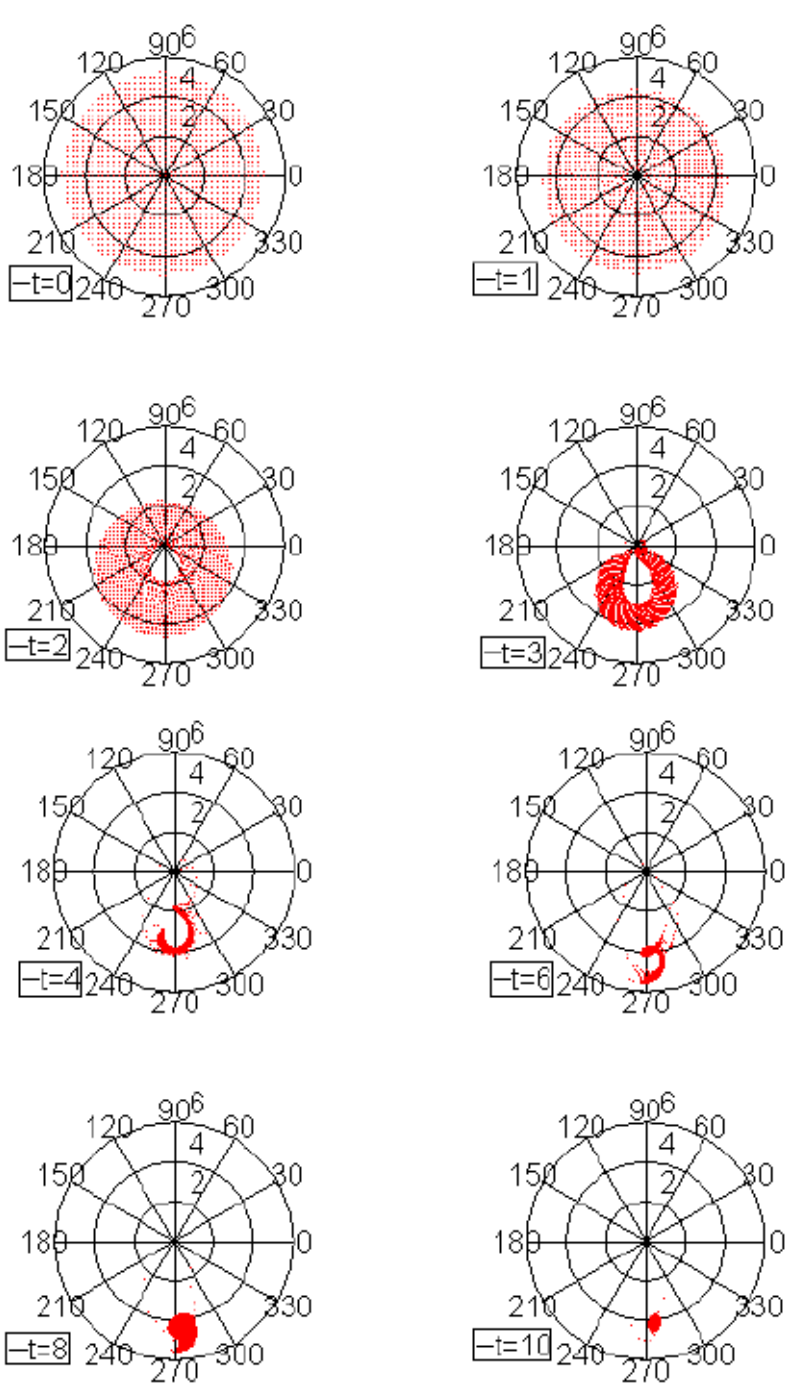

Figure 2: Temporal evolution of the distribution of identical droplets near a horizontal vortex with axial stretching.

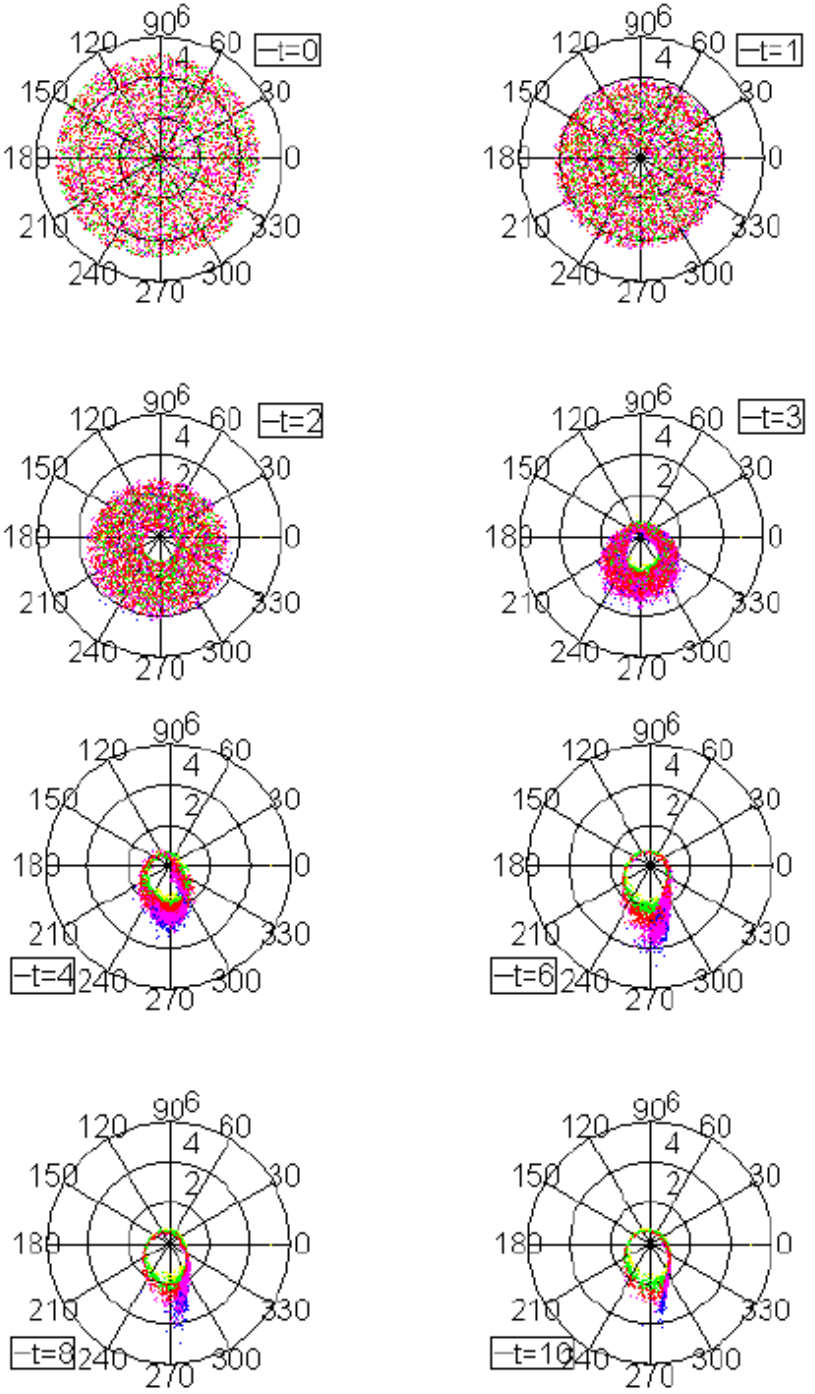

Figure 4: Temporal evolution of the distribution of droplets with gaussian spectrum near a horizontal vortex with axial stretching.

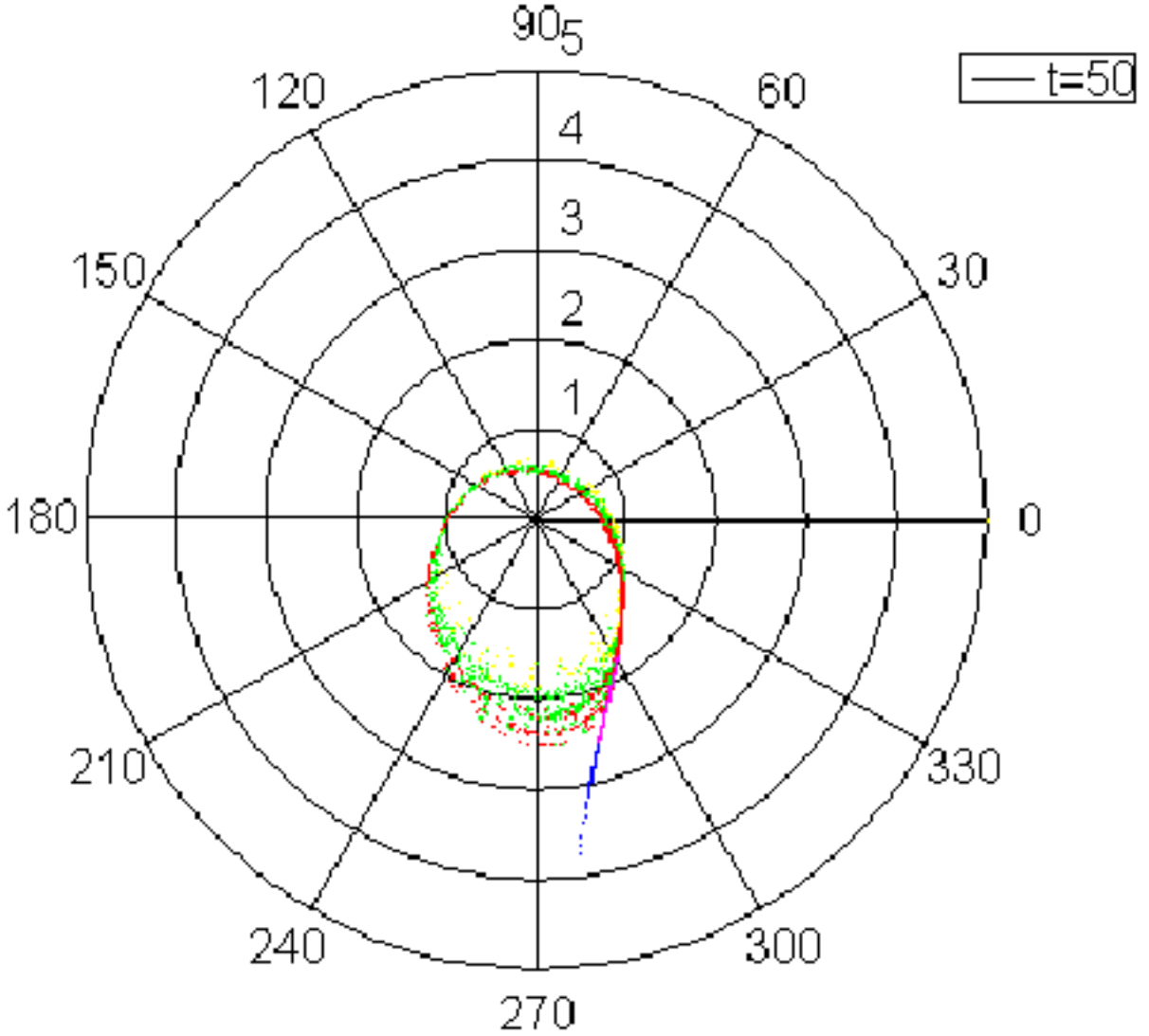

Figure 5: Distribution of droplets with gaussian spectrum after 2.5 turnover times of the vortex. Initial distribution was spatially uniform.

$$\begin{cases} \ddot{r} - r\dot{\phi}^2 = a(-\frac{\gamma}{2}r - \dot{r}) \\ 2\dot{r}\dot{\phi} + r\ddot{\phi} = a(\frac{\Gamma}{2\pi r} - r\dot{\phi}) \\ \ddot{z} = a(\gamma z - \dot{z}) - g \end{cases}$$

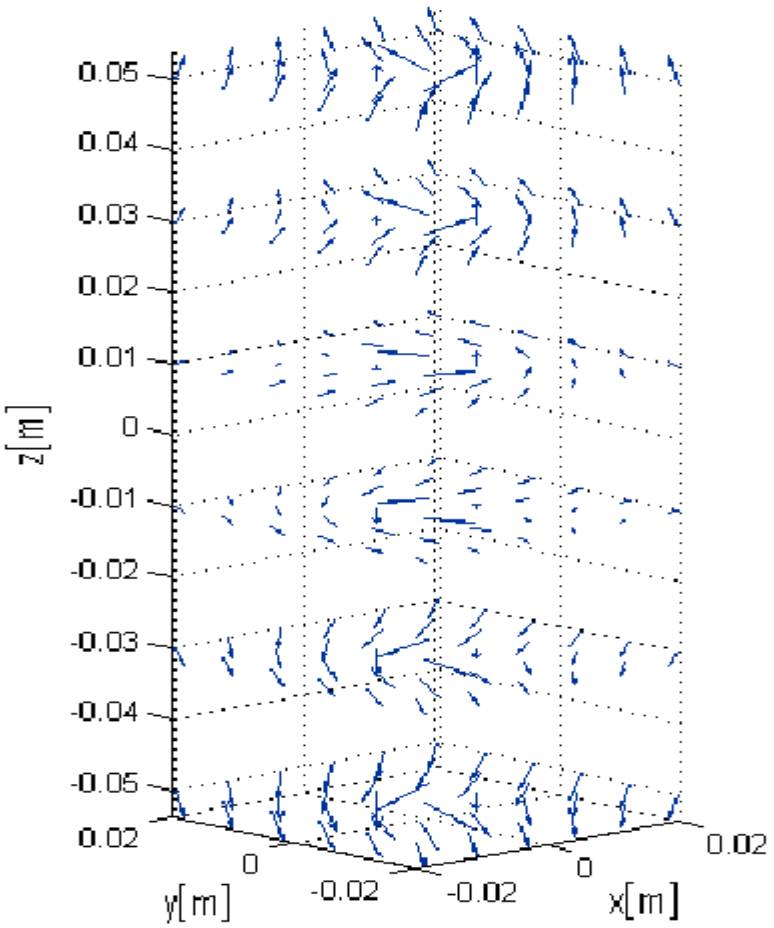

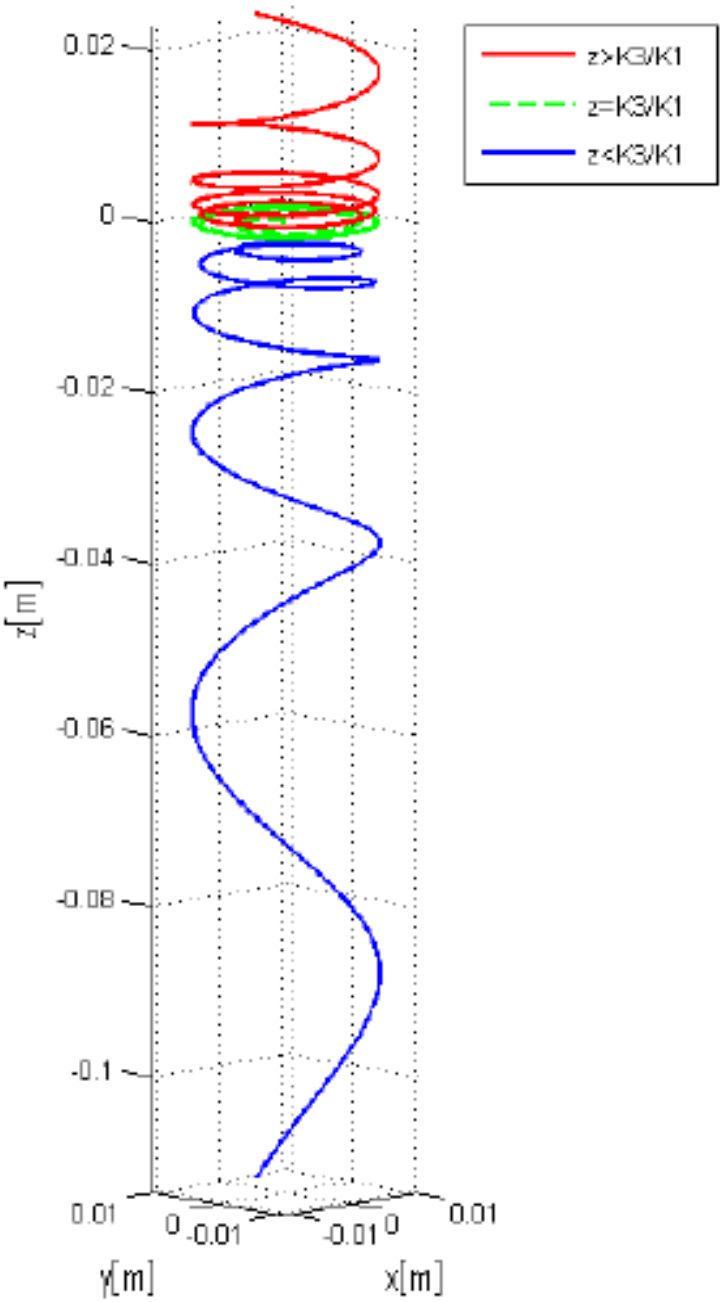

K. Karpinska M.Sc. thesis

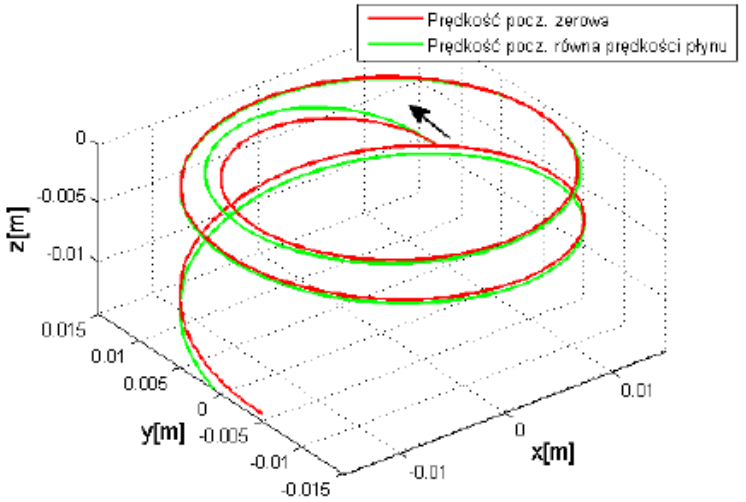

(a) $r_0 = 5\ mm$

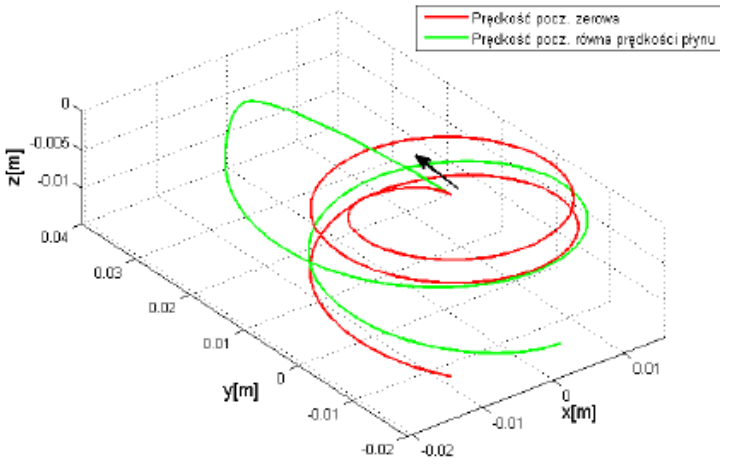

(b) $r_0 = 1\ mm$

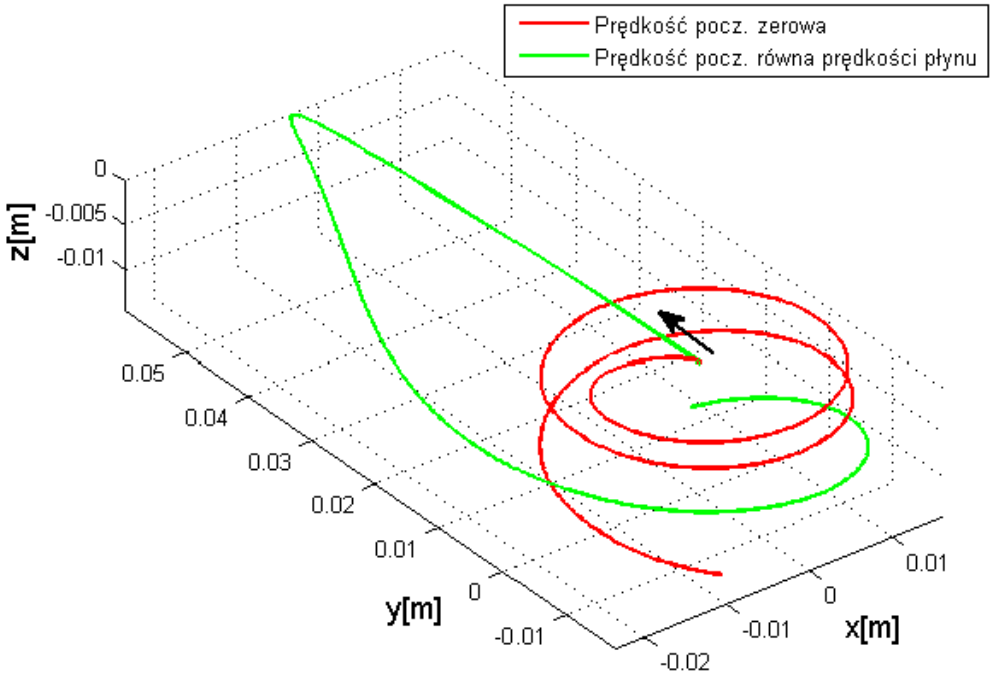

(c) $r_0 = 0.5\ mm$

"Sling effect"
red – initial velocity of the droplet equal to this of fluid

green – initial velocity of the droplet zero

Inclined vortex

$$\vec{F}_g = -mg(sin(\theta)\hat{e_y} + cos(\theta)\hat{e_z}) = -mg(sin(\theta)sin(\phi)\hat{e_r} + sin(\theta)cos(\phi)\hat{e_\phi} + cos(\theta)\hat{e_z}).$$

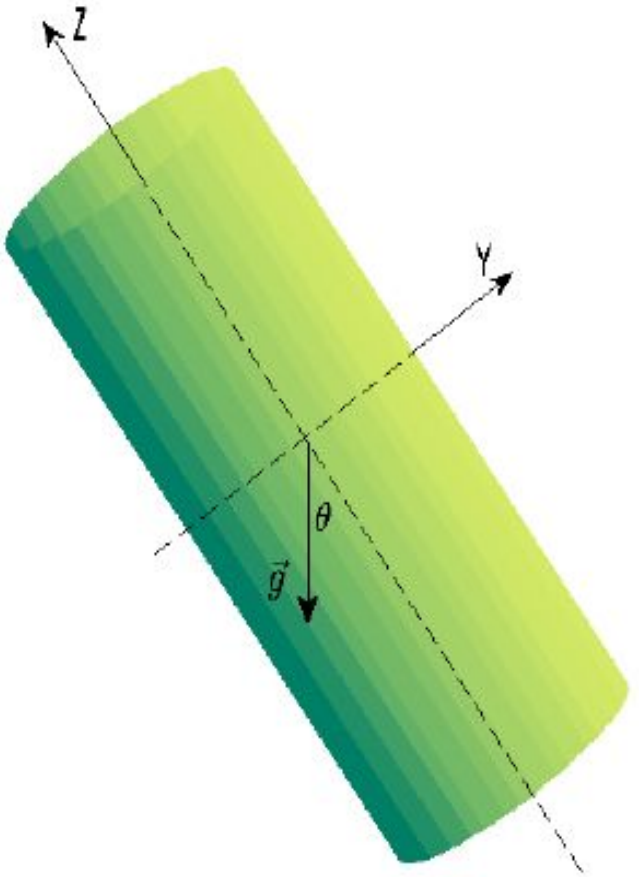

$$\begin{cases} \ddot{r} - r\dot{\phi}^2 = a(-\frac{\gamma}{2}r - \dot{r}) - gsin(\theta)sin(\phi) \\ 2\dot{r}\dot{\phi} + r\ddot{\phi} = a(\frac{\Gamma}{2\pi r} - r\dot{\phi}) - gsin(\theta)cos(\phi) \\ \ddot{z} = a(\gamma z - \dot{z}) - gcos(\theta) \end{cases},$$

After scaling (non dimensional equations)

$$\begin{cases} \ddot{r} - r\dot{\phi}^2 = -(\frac{\gamma}{2a}r + \dot{r} + \frac{g}{Sa^2}sin(\theta)sin(\phi)) \\ 2\dot{r}\dot{\phi} + r\ddot{\phi} = \frac{1}{r} - r\dot{\phi} - \frac{g}{Sa^2}sin(\theta)cos(\phi)) \\ \ddot{z} = \frac{\gamma}{a}z - \dot{z} - \frac{g}{Sa^2}cos(\theta) \end{cases}$$

$$K_1 = \frac{\gamma}{a} = L_1,$$
$$K_2 = \frac{g}{Sa^2}cos(\theta) = L_2cos(\theta),$$
$$K_3 = \frac{g}{Sa^2}sin(\theta) = L_2sin(\theta),$$

$$\begin{cases} \ddot{r} - r\dot{\phi}^2 = -(\frac{K_1}{2}r + \dot{r} + K_3sin(\phi)) \\ 2\dot{r}\dot{\phi} + r\ddot{\phi} = \frac{1}{r} - r\dot{\phi} - K_3cos(\phi)) \\ \ddot{z} = K_1z - \dot{z} - K_2 \end{cases}$$

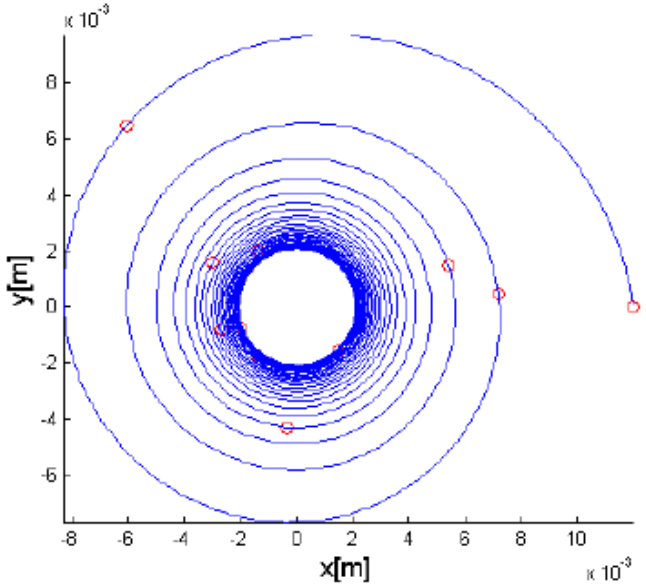

(a) R=2.5 μm

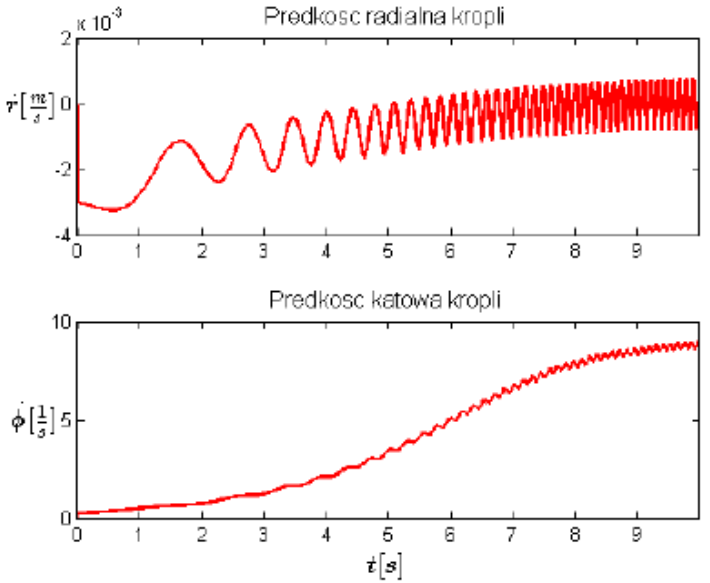

(b) R=2.5 μm

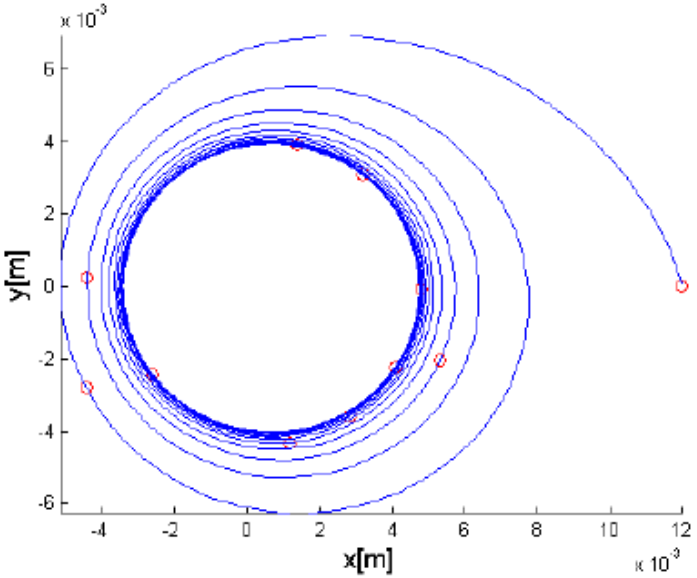

(c) R=9 μm

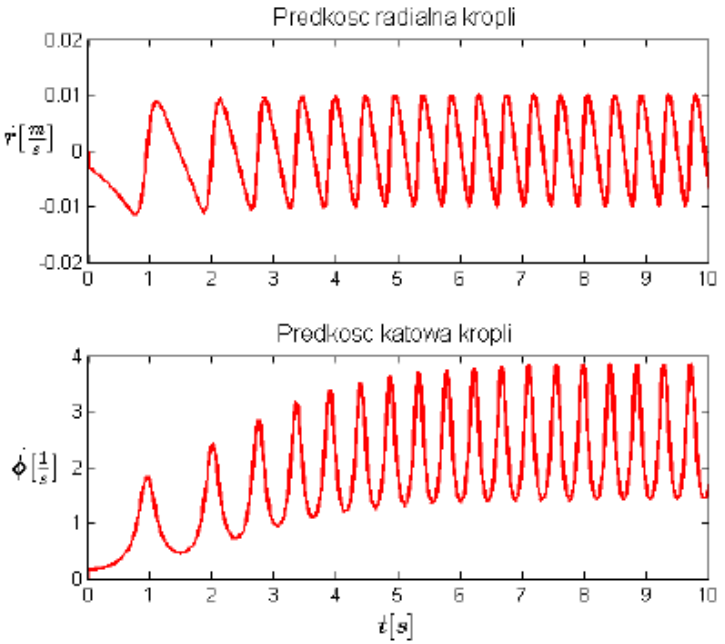

(d) R=9 μm

Rysunek 3.7: Trajektorie i predkości ruchu kropel o promieniu R w wirze ukośnym o $\gamma = 0.5$, $L_w = 2.5 \cdot 10^{-4}$, $\theta = 0.45\pi$

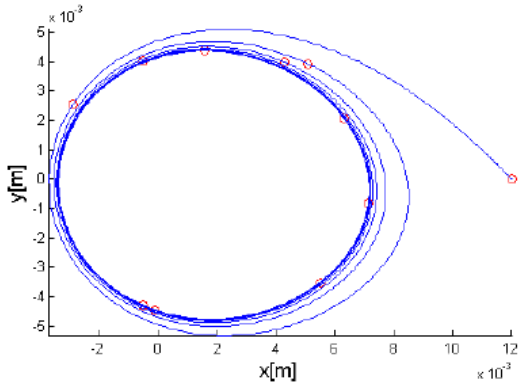

(a) R=12 μm

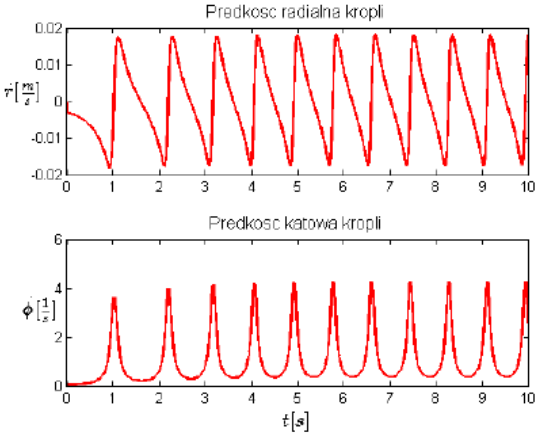

(b) R=12 μm

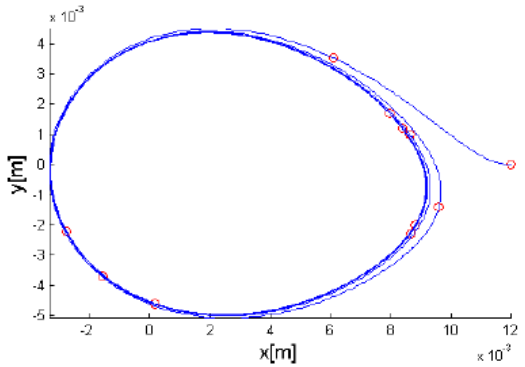

(c) R=13 μm

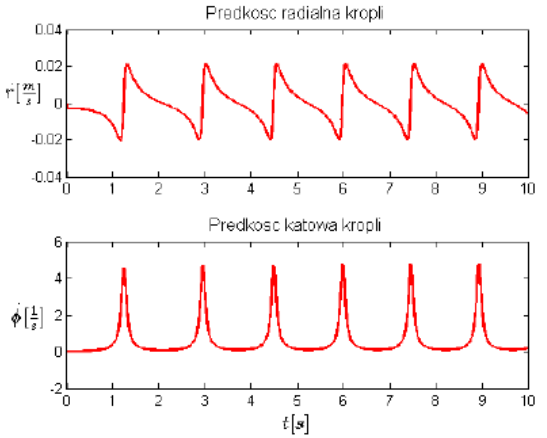

(d) R=13 μm

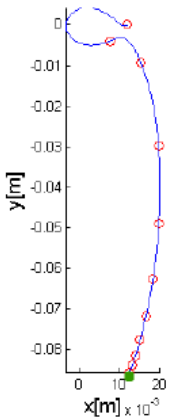

(e) R=13.5 μm

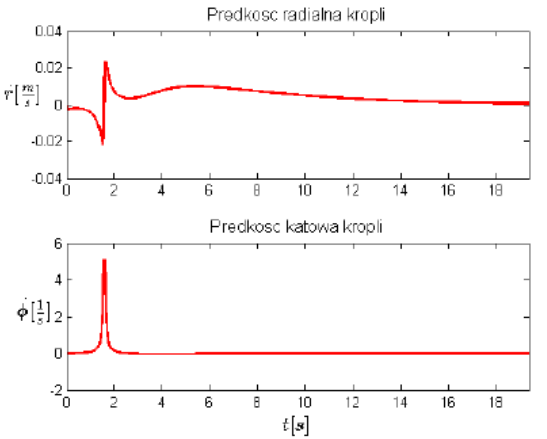

(f) R=13.5 μm

Rysunek 3.8: Trajektorie i predkości ruchu kropel o promieniu R w wirze ukośnym o $\gamma = 0.5$, $L_w = 2.5 \cdot 10^{-4}$, $\theta = 0.45\pi$.

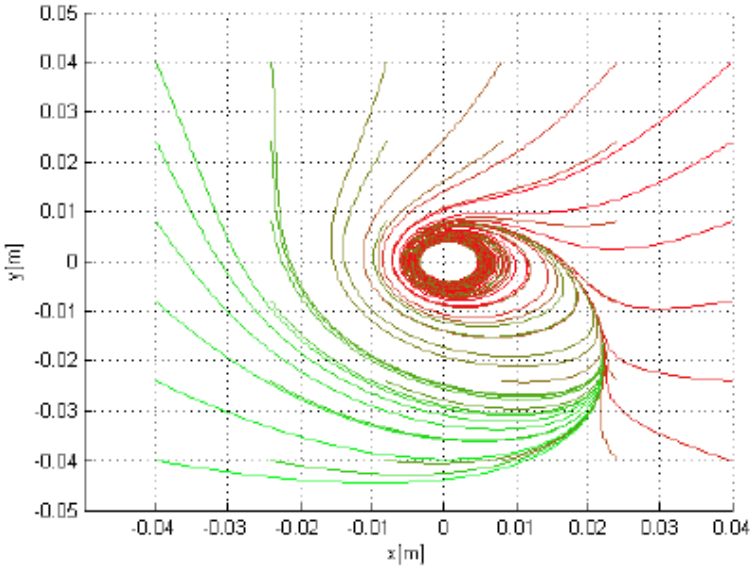

(a) R=9 μm

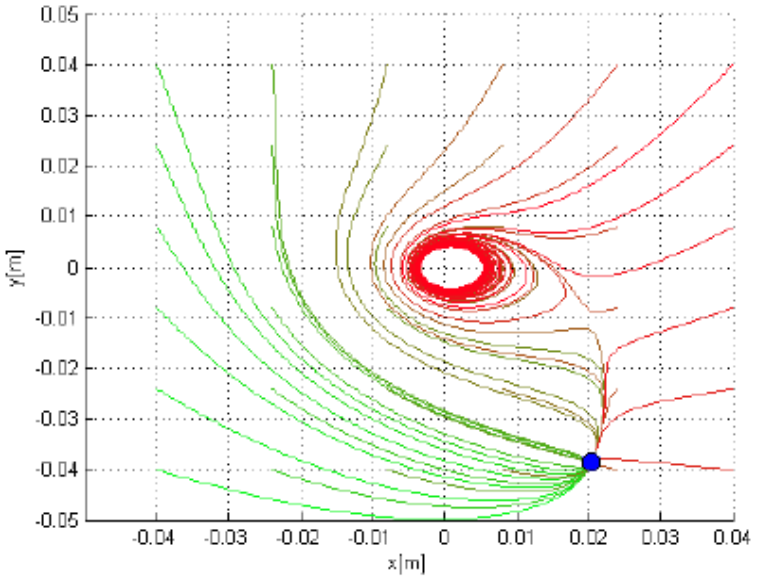

(b) R=10 μm

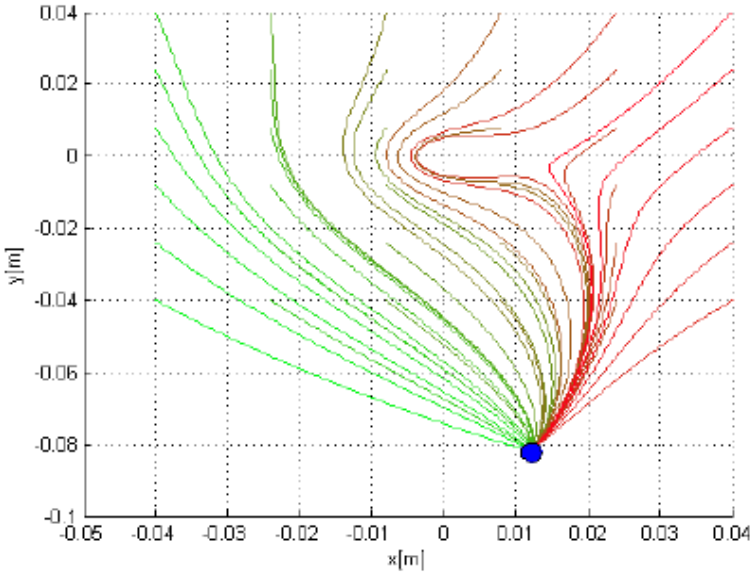

(c) R=13 μm

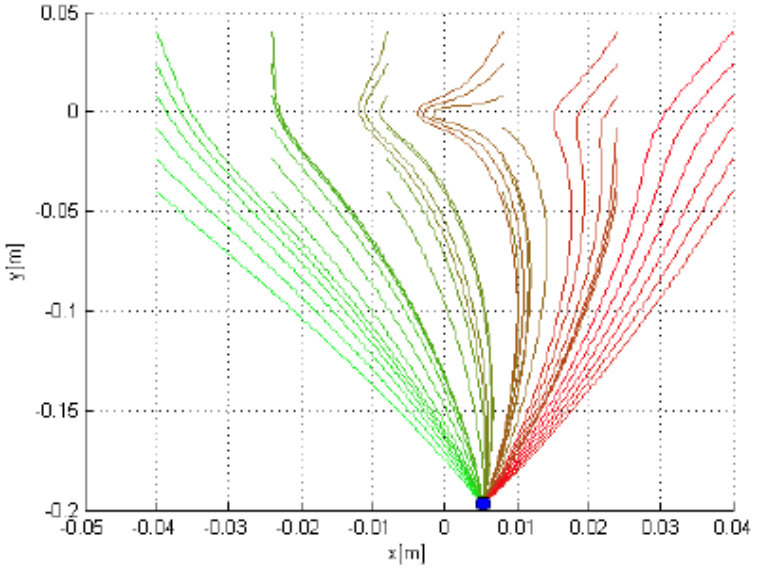

(d) R=20 μm

Rysunek 3.9: Zbiory trajektorii 36 kropel rozmieszczonych równomiernie w płaszyźnie równowagi $z = K3/K1$, na kwadracie o boku l=8cm, wokół osi wiru o promieniach R w wirze ukośnym o $\gamma = 0.5$, $L_w = 2.5 \cdot 10^{-4}$, $\theta = 0.45\pi$.

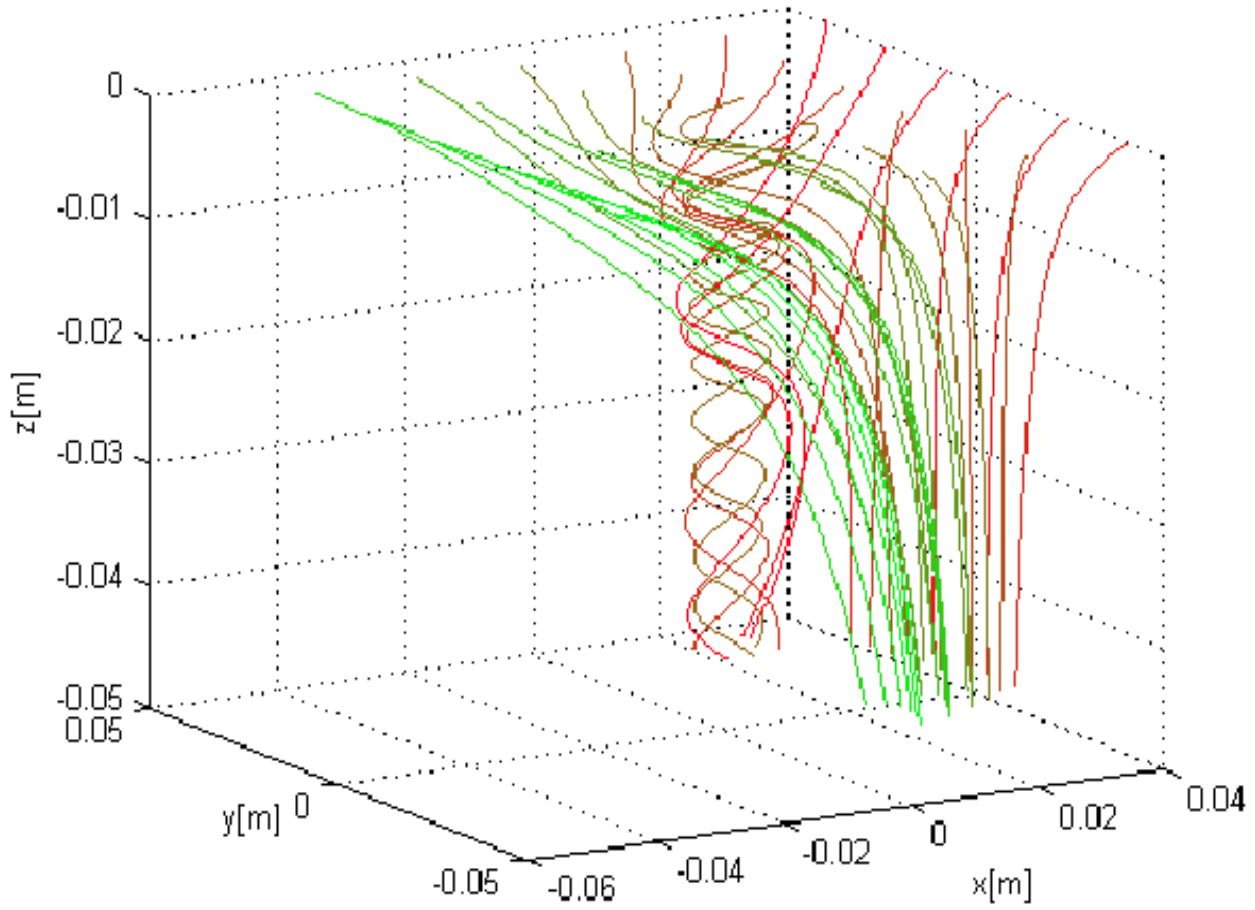

Rysunek 3.11: Zbiory trajektorii 36 kropel rozmieszczonych równomiernie w płaszyźnie $z_0 = 0$, na kwadracie o boku l=8cm wokół osi wiru, o promieniach $R = 10\mu m$, w słabym wirze ukośnym przy $\theta = 0.45\pi$.